

MARION PAOLA FLORA CHARPENTIER

Evaluation of bacterial behaviour of porous activated carbon obtained from black liquor processing with silver nanoparticles for bone regeneration application.

São Paulo  
2019



# Evaluation of bacterial behaviour of porous activated carbon obtained from black liquor processing with silver nanoparticles for bone regeneration application.

Marion Paola Flora CHARPENTIER

Master of Sciences Thesis (INSA)  
Graduation project (USP)  
Material Science Engineering

Under the supervision of:  
Prof. Dr. Guilherme Frederico Bernardo Lenz e Silva  
Co-supervision :  
Dr. Patrícia de Almeida Mattos

Escola Politécnica da USP  
Departamento de engenharia metalúrgica e de materiais  
São Paulo, Brazil



**DEPARTAMENTO DE ENGENHARIA  
METALÚRGICA E DE MATERIAIS**

Escola Politécnica da Universidade de São Paulo

INSA de Lyon  
Département science et génie des matériaux  
Lyon, France



**INSA**

INSTITUT NATIONAL  
DES SCIENCES  
APPLIQUÉES  
LYON

São Paulo, 2019



Autorizo a reprodução e divulgação total ou parcial deste trabalho, por qualquer meio convencional ou eletrônico, para fins de estudo e pesquisa, desde que citada a fonte.

#### Catálogo-na-publicação

Charpentier, Marion Paola Flora

Evaluation of bacterial behaviour of porous activated carbon obtained from black liquor processing with silver nanoparticles for bone regeneration application. / M. P. F. Charpentier; Lenz e Silva, Guilherme F. B. (orientador) -- São Paulo, 2019.

79 p.

Trabalho de Formatura - Escola Politécnica da Universidade de São Paulo. Departamento de Engenharia Metalúrgica e de Materiais.

1.Composites 2.Bone regeneration 3.Activated carbon 4.Silver nanoparticles I.Universidade de São Paulo. Escola Politécnica. Departamento de Engenharia Metalúrgica e de Materiais II.t.



## Thanks

I would like to thank my supervisor, Prof. Dr. Guilherme Frederico Bernardo Lenz e Silva, for the quality of his supervision, his patience, for the acknowledgment shared and for the opportunity to present this work in the 63<sup>th</sup> Congress of Ceramics in Bonito/Brazil.

I would like to thank my co-supervisor, Patricia Almeida, for her implication in this work, for her accessibility to help at any time and her solicitude.

I would like to thank Gisele Amaral-Labat, for sharing her experience in activated carbon synthesis and characterization and for her sympathy.

I would like to thank Caio Zuccolan Carvas, Ana Pupim, Danyela Cardoso Carvalho and Daniel Luiz Rodrigues Junior for their assistance and friendship all along this work.

I would like to thank Jarir Mahfoud, Alain Fave, Xavier Kleber, Samuel Toffoli and Antonio Carlos Coelho for the opportunity to study at the University of São Paulo in the Materials Science Engineering Department.

I would like to thank my parents Véronique and Laurent for their comprehension, support and love.

I would like to thank Valeria and Ewandro for their solicitude and their presence in my daily life.

Finally, I would like to thank Thiago for his encouragements and kindness.

To all these people, I present my thanks, my gratitude and my respect.



## Abstract

**Title:** Evaluation of bacterial behaviour of porous activated carbon obtained from black liquor processing with silver nanoparticles for bone regeneration application.

**Keywords:** activated carbon, bone repair, antibacterial activity of silver nanoparticles, lignin waste, biomaterial composite.

**Author:** CHARPENTIER, Marion Paola Flora

Carbon structures are a center of interest in the biomedical area due to their biocompatibility and for their structure, which can be modified according to the application. Indeed, it has been proved that porous activated carbon, thanks to its structural properties, can enhance cell growth and vascularization, two essential processes in bone regeneration.

Actually, after a bone surgery, infection is still recurrent in the local of surgery and there is a huge necessity to solve this problem. To reduce infection, one of the possible solutions could be to integrate silver nanoparticles to a scaffold as they are well known for their antibacterial properties.

In this work, a waste of cellulose paper industry, pure black liquor, was used as a precursor for activated carbon. Silver nanoparticles were added on the surface of the porous activated carbon by adsorption process. The aim of this work was to find the best conditions of process to obtain a biomaterial that enhances cell regeneration and that minimizes infection after implantation. During carbonization, several temperatures and atmospheres were used and the influence of these parameters on structure and composition was analysed. Then, the different activated carbon samples were impregnated with silver nanoparticles solutions, prepared in different concentrations in order to evaluate the influence, not only of the activated carbon structure and composition but also of the quantity of silver nanoparticles, on the adsorption and delivery processes and on antibacterial properties. In order to evaluate the antibacterial efficiency, the samples were tested on *E.Coli*.



It can be observed that different temperatures and atmospheres result in different structures: higher temperature and the use of CO<sub>2</sub> permit to obtain larger porous. Composites of activated carbon and silver nanoparticles were proved to be efficient to reduce *E.Coli* bacterial growth.



## Résumé

**Titre:** Evaluation de l'action antibactérienne de charbons actifs poreux synthétisés à partir de liqueur noire et imprégnés avec des nanoparticules d'argent pour de futures applications en régénération osseuse.

**Mots clés :** Charbon actif, réparation osseuse, activité antibactérienne de nanoparticules d'argent, résidu de lignine, biomatériau composite.

Les structures de carbone se sont placées au centre de la recherche dans le domaine biomédical de part leur biocompatibilité et leur structure, qui est modulable en fonction de l'application souhaitée. En effet, il a été prouvé que les structures poreuses à base de carbone, de part leur structure, peuvent accélérer la croissance cellulaire et la vascularisation, deux processus essentiels à la réparation osseuse.

Actuellement, suite à une chirurgie osseuse, il est courant qu'une infection s'ensuive et il est plus que nécessaire de trouver une solution à ce problème. Afin de réduire l'infection, une possible solution est d'intégrer des nanoparticules d'argent à la surface du scaffold puisqu'elles possèdent des propriétés antibactériennes.

Au sein de ce projet, un résidu provenant des fabriques de papier, la liqueur noire, a été utilisée sans subir de transformations comme précurseur pour l'obtention de charbon actif. Des nanoparticules d'argent ont été additionnées à la surface du charbon actif poreux par adsorption. Le but de ce travail est de déterminer les meilleures conditions de procédé afin d'obtenir un biomatériau capable d'accélérer la régénération osseuse tout en minimisant l'infection après implantation. Pendant le processus de carbonisation plusieurs températures et atmosphères ont été utilisées afin de déterminer l'influence de ces paramètres sur la structure et la composition du charbon actif. Ensuite, les différents échantillons de charbon actif ont été imprégnés avec des solutions de nanoparticules d'argent en concentrations différentes pour évaluer l'influence de la concentration de la solution croisée avec les propriétés de chaque type de charbon actif sur les processus d'adsorption, de libération et sur les propriétés antibactériennes résultantes. Afin



d'évaluer l'efficacité antibactérienne, les échantillons ont été testés avec des cultures de *E.Coli*.

Il a été observé que la température et le type d'atmosphère influencent la structure obtenue: en augmentant la température et en remplaçant l'argon par du CO<sub>2</sub>, des pores plus larges sont obtenus. Les composites de charbon actif avec nanoparticules d'argent montrent une réduction de la croissance bactérienne de *E. Coli*.



## Resumo

**Título:** Avaliação da ação antibacteriana de um carvão ativado poroso sintetizado a partir de licor negro e impregnado com nanopartículas de prata para fins de uso em regeneração óssea.

**Palavras chaves:** Carvão ativado, reparação óssea, atividade antibacteriana de nanopartículas de prata, resíduo de lignina, biomaterial compósito.

Estruturas de carbono tornaram-se um grande centro de interesse na área biomédica graças à biocompatibilidade e à estrutura delas em si, que pode ser modificada em função da aplicação desejada. De fato, foi comprovado que a estrutura do carvão ativado poroso pode acelerar o crescimento celular e a vascularização, dos processos essenciais à regeneração óssea.

Actualmente, depois de uma cirurgia óssea, é comum a ocorrência de processos infecciosos no sítio cirúrgico e tem uma grande necessidade de solucionar esse problema. Para reduzir a infecção, uma possível solução é de integrar nanopartículas de prata, conhecidas por suas propriedades antibacterianas, à estrutura matriz.

Ao longo desse projeto, um resíduo do processo de fabricação de papel, o licor negro, foi reaproveitado como precursor para a obtenção de carvão ativado. Nanopartículas de prata foram adicionadas na superfície do carvão ativado poroso por processo de adsorção física. O objetivo deste trabalho é de achar as melhores condições de processo para obter um biomaterial que melhora a regeneração óssea e que minimize os riscos de infecção após implantação. Para o processo de carbonização, diferentes temperaturas e atmosferas foram utilizadas e a influência desses parâmetros sobre estrutura e composição foi analisada. Em seguida, as amostras de carvão ativado foram impregnadas com soluções de nanopartículas de prata, preparadas com diferentes concentrações, para analisar a influência da concentração, cruzada com a influência das características de cada carvão sintetizado, nos processos de adsorção e de liberação de nanopartículas de prata.



bem com nas propriedades antibacterianas. Para a avaliação da eficiência antibacteriana, as amostras foram testadas com *E. Coli*.

Foi observado que as diferentes temperaturas e atmosferas resultam em estruturas diferentes: temperaturas mais elevadas e o uso de CO<sub>2</sub> demonstraram maior tamanho de poro. A associação de nanopartículas de prata com carvão ativado resultem na diminuição do crescimento de *E. Coli*.



# Goals

## 1. General

In this work, the principal focus is to develop a carbonaceous material impregnated with a bactericidal agent (silver nanoparticles) in order to use it for bone repair applications.

## 2. Specific

More specifically, the all project, aim at:

- recycling a by-product of the Kraft process producing activated carbon,
- an engineered production of an extremely porous carbonaceous material that has the capacity to adsorb nanoparticles,
- and testing the bactericidal efficiency of an extremely porous material impregnated of silver nanoparticles.



# Table of contents

<b>Theoretical background</b>	17
Carbon and activated carbon	12
Characteristics, properties and main uses	12
Manufacturing process	13
The different forms of activated carbon	15
Market of activated carbon	15
Black liquor	16
Characteristics	16
Principal uses	17
Biomedical properties of lignocellulosic materials	17
Market of black liquor and lignin	18
Nanosilver particles	19
Characteristics	19
Manufacturing process	19
Antibacterial mechanism	20
Silver nanoparticles drug delivery	22
Environmental, health and safety issues of silver nanoparticles	23
Principal uses	24
Tissue engineering	25
Biomaterials used in tissue engineering	26
Regeneration process	26
Bone regeneration	26
Techniques of characterization	27
Scanning electron microscope (SEM) with Energy Dispersive X-Ray Spectroscopy (EDX)	27
Spectrophotometry	28
Dynamic light scattering (DLS)	29
<b>Materials and methods</b>	30
Synthesis of activated carbon	30
Polymerization of the material	30
Materials	30
Process	31
Carbonization	33
Materials	34
Process	34
Washing	36
Materials	36
Process	36
Drying	37
Materials	37
Process	37



Impregnation with silver nanoparticles	38
Preparation of the solution of nanosilver particles	38
Materials	38
Process	39
Evaluation of the adsorption and desorption of nanosilver particles by the samples of activated carbon	40
First experiment:	41
Materials	41
Process	41
Second experiment:	42
Materials	42
Process	42
Evaluation of the bactericidal activity	44
Materials	44
Process	44
Characterization techniques	46
<b>Results</b>	46
Activated carbon structure and composition in different conditions of carbonization	47
Structure analysis	47
Composition analysis	49
Characterization of silver nanoparticles	50
Nanosilver particles size distribution	50
Antibacterial activity of the nanosilver solutions	51
Analysis over the composite of activated carbon and nanosilver particles	55
Analysis of the silver nanoparticles adsorption by activated carbon samples using spectrophotometry	55
Spectrophotometry analysis to see if silver nanoparticles are liberated by activated carbon samples using	56
Analysis of the silver nanoparticles adsorption by activated carbon samples using SEM analysis	60
Antibacterial activity of the activated carbon/ AgNPs composite	65
<b>Discussion of the results</b>	69
<b>Conclusion</b>	71
<b>Bibliography</b>	73



## List of figures

Figure 1: Structure of activated carbon materials. Adapted from [2].	12
Figure 2: Reaction mechanisms during carbonization. Adapted from [7].	13
Figure 3: The different mechanisms of activation. Adapted from [8].	13
Figure 4: The different manufacturing processes to obtain activated carbon.	14
Figure 5: the different forms of activated carbon. Figure adapted from [9].	15
Figure 6: Papermaking process flowchart. Adapted from [11].	16
Figure 7: Synthetic view of the application of the lignocellulosic feedstock. Adapted from [13], copyright WILEY-VCH Verlag GmbH & Co. KGaA, Weinheim.	17
Figure 8: Chemical representation of a possible structure of a lignin. Adapted from [6].	18
Figure 9: Possible uptake process and cytotoxic mechanism induced by nanosilver particles. Adapted from [19].	22
Figure 10: The different mechanisms that influence silver ions release. Adapted from [27].	23
Figure 11: Sources of Ag NPs exposure and their adverse effects. Adapted from [31].	24
Figure 12: Applications of silver nanoparticles. Adapted by the author.	25
Figure 13: Scheme of bone regeneration process. Adapted from [39].	27
Figure 14: Structure of a SEM-EDX device. Adapted from [41].	28
Figure 15: Basic structure of a spectrophotometer. Adapted from [42].	28
Figure 16: Basic structure of a DLS. Adapted from [43].	29
Figure 17: Reaction mechanism of lignin and resorcinol with formaldehyde under alkaline conditions. Adapted from [7].	30
Figure 18: Mixture of all the reagents for the polymerization.	32
Figure 19: Beginning of the polymerisation.	32
Figure 20: Polymerized precursor of activated carbon.	33
Figure 21: Descriptive scheme of the over GRION Fornos Industriais.	34
Figure 22: Sample 1, a) before carbonization with argon at 1000 °C, b) after carbonization with argon at 1000 °C.	35
Figure 23: Description of the washing system.	37



Figure 24: On the left, photograph of the oven used for the drying step. On the right (inside the oven), petri dishes containing the samples wrapped in filter paper.....	38
Figure 25: Solution of nanosilver particles.....	40
Figure 26: Organization of the the tissue culture plate used for the test of the AgNPs solution.....	45
Figure 27: a) AC-Ar-800 °C, x150; b) AC-Ar-1000 °C, x150; c) AC-CO2-800 °C, x150; d) AC-Ar-800°C, x500; e) AC-Ar-1000 °C, x600; f) AC-CO2-800 °C, x600. ...	48
Figure 28: Composition of the sample of activated carbon, after carbonization with argon at 800 °C. ....	49
Figure 29: Composition of the sample of activated carbon, after carbonization with argon at 1000 °C. ....	50
Figure 30: Composition of the sample of activated carbon, after carbonization with CO2 at 800 °C.....	50
Figure 31: Size distribution of the silver nanoparticles in the solution 27 ppm concentrated. ....	51
Figure 32: Details of the size distribution of the silver nanoparticles. ....	51
Figure 33: Tissue culture plate used to test the chemical AgNPs solution of 27ppm and its disposition.....	52
Figure 34: Results of the analysis given by the spectrophotometer. ....	52
Figure 35: Tissue culture plate used to test AgNPs solutions of 27ppm / 54ppm / 81ppm and its disposition.....	53
Figure 36: Results of the analysis given by the spectrophotometer. ....	54
Figure 37: Average reduction of bacterial growth treating with AgNPs solutions of 27 ppm, 54 ppm and 81 ppm. ....	54
Figure 38: Absorbances as a function of time for the initial solution of 27 ppm of silver nanoparticles containing the different samples of activated carbon. ....	56
Figure 39: Absorbance as a function of time for physiological solutions containing activated carbon/ AgNPs composite samples at a) 37°C, b) pH 6.5, c) pH 7, d) pH 7.4. ....	58
Figure 40: Illustrative scheme explaining the formation of AgCl. Adapted from [48]	59
Figure 41: SEM-EDX analysis of CA/AgNPs (81 ppm solution) carbonized at 1000 °C with argon after immersion in physiological solution at 37°C in pH 7.4. ....	59
Figure 42: SEM-EDX analysis of CA/AgNPs (54 ppm solution) carbonized at 800 °C with argon after immersion in physiological solution at 37°C in pH 7.4. ....	59



Figure 43: SEM-EDX analysis of CA/AgNPs (81 ppm solution) carbonized at 800 °C with argon after immersion in physiological solution at 37°C in pH 7.4. ....	60
Figure 44: SEM image of activated carbon samples impregnated with 81ppm solution of nanosilver particles, magnification x1500, of a) AC-Ar-800 °C ;b) AC-Ar-1000 °C ;c) AC- CO2-800 °C.....	61
Figure 45: EDX analysis of the AgNPs on the surface of the sample of activated carbon carbonized with argon at 1000 °C impregnated with the 54 ppm solution. ...	62
Figure 46: Tissue culture plate used to test activated carbon samples impregnated with the 27 ppm solution.....	65
Figure 47: Spectrophotometry results of the tissue culture plate used to test activated carbon samples impregnated with the 27 ppm solution.....	66
Figure 48: Tissue culture plate used to test activated carbon samples impregnated with the 54 ppm and 81ppm solution.....	67
Figure 49: Spectrophotometry results of the tissue culture plate used to test activated carbon samples impregnated with the 54 ppm and 81 ppm solution.....	67
Figure 50: SEM image of activated carbon carbonized at 800 °C with argon and impregnated by the 81 ppm solution. Magnification x40 000.....	68



## List of tables

Table 1: A possible composition of black liquor. Adapted from [12].	17
Table 2: Comparison between the different methods for the synthesis of Ag-NPs...	20
Table 3: List of reagents for the polymerization.	30
Table 4: Materials used for the synthesis of the polymer.	31
Table 5: Weight of the different reagents for the polymerization of black liquor.	31
Table 6: Carbonization conditions of the samples of activated carbon.	34
Table 7: Weighs of the samples, before and after the carbonization.	35
Table 8: Reagent used in the silver nanoparticle synthesis.	38
Table 9: Mass of reagents weighted to prepare the silver nanoparticles solution.	39
Table 10: Reagents used in the first experiment.	41
Table 11: Content of each tube for the first experiment.	42
Table 12: Reagents used in the second experiment during the adsorption phase.	43
Table 13: Description of the desorption experiment for the activated carbon carbonized with argon at 800 °C.	43
Table 14: Description of the desorption experiment for the activated carbon carbonized with argon at 1000 °C.	44
Table 15: Description of the desorption experiment for the activated carbon carbonized with CO <sub>2</sub> at 800 °C.	44
Table 16: Average pore diameter ( $\Phi_m$ ) of the different samples of activated carbon.	49
Table 17: SEM observations with high contrast after the adsorption of AgNPs by the samples of activated carbon.	63
Table 18: Results of the Image J processing of the SEM images of the activated carbon samples after impregnation with solution of 54 ppm and 81 ppm of silver.	64



# I. Theoretical background

## A. Carbon and activated carbon

### 1. Characteristics, properties and main uses

Activated carbon (AC), also called active carbon or activated charcoal is distinct from charcoal and from carbon. With an unit structure similar to the graphite's one; the global structure of activated carbon is similar to a very porous stack of carbon foils where the foils are highly disorganized. That's why activated carbon structure is classified as amorphous [1].

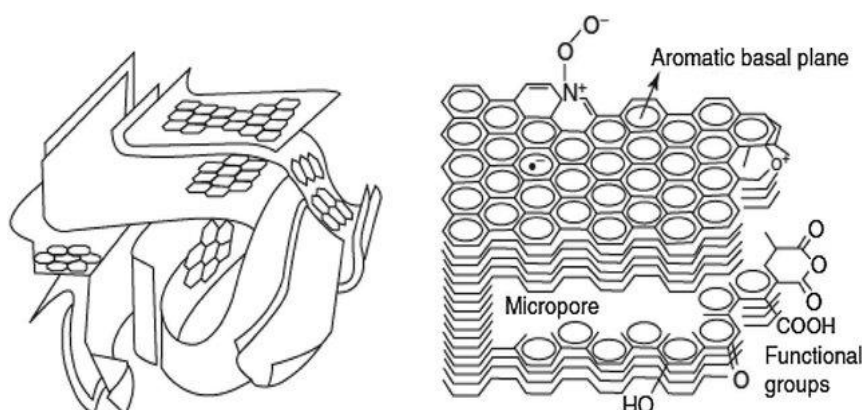


Figure 1: Structure of activated carbon materials. Adapted from [2].

To make activated carbon, raw materials that have a high percentage of carbon in their composition and a low amount of inorganic substances are necessary. Consequently, to achieve these criteria, it is generally used degraded, fossil or fresh biomass. The properties of the activated carbon, such as surface area, total volume of porous, size distribution of porous and surface chemistry totally depend on the raw material and on the process of fabrication [3,4]. With a very large surface area, the activated carbon has excellent adsorption properties [3,5] in addition to its good properties in term of thermal and electrical conduction.

Adsorption is a phenomenon where the molecules fixe themselves at the surface of the adsorbent forming week bounds such as hydrogen bonds, Van der Waals forces and electrostatic interactions. Thank to this adsorption capacity, activated carbon is a centre of interest in many areas counting gas purification, water



treatment, deodorization, food and beverage industry, energy storage medicine and more [3].

## 2. Manufacturing process

To produce activated carbon, it is necessary to have a carbonaceous material available. Various materials fit this criteria such as any type of wood, coal, nutshells but also peat or pure black liquor [3]. Currently, there are two industrial processes to produce activated carbon.

The first one uses physical activation. This method has two steps : carbonization and activation [1,3,4,6]. During the carbonization step the carbonaceous material is pyrolysed between 600 °C and 1000 °C in an inert atmosphere, under argon or nitrogen environment. During this step, all the non-carbonaceous species are removed producing a material with high percentage of carbon.

Then comes the activation where the carbonised material is oxidized, generally with CO<sub>2</sub>, or steam, in a temperature range of 600 °C-1200 °C. The development of porosity is due to the penetration of the oxidative agent inside the intern structure that will remove some carbon atoms converting them into gas. The reaction mechanisms are the following ones [7]:

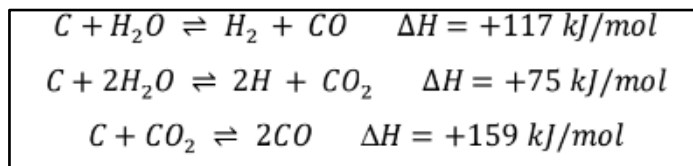


Figure 2: Reaction mechanisms during carbonization. Adapted from [7].

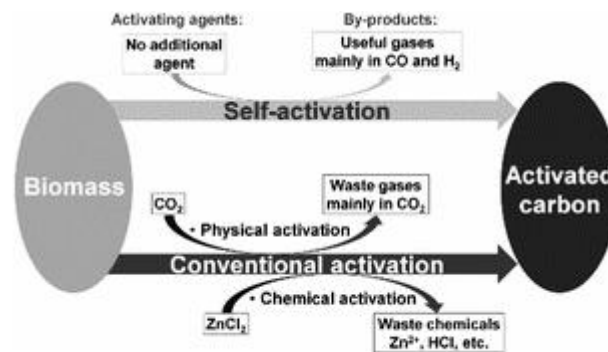


Figure 3: The different mechanisms of activation. Adapted from [8].



The second process uses chemical activation which consists in chemical impregnation followed by carbonization [1,3,4]. For the chemical impregnation, after grinding the carbonaceous material, acids such as phosphoric acid, bases like potassium hydroxide, sodium hydroxide or salts like zinc chloride can be used. After the impregnation it is necessary to pyrolyse the material between 400 °C and 900 °C and then to wash it in order to liberate the porous and remove the activation agents. The final step is to dry the activated carbon.

This process is preferred over physical activation because it doesn't need high temperature process and it is way faster. It can also be used when it is required to adsorb big molecules by developing mesoporosity which can be reinforced by controlling the degree of impregnation (advanced impregnation results in bigger pores).

After the synthesis, an additional step of functionalization can be realized to enhance adsorption of specific molecules.

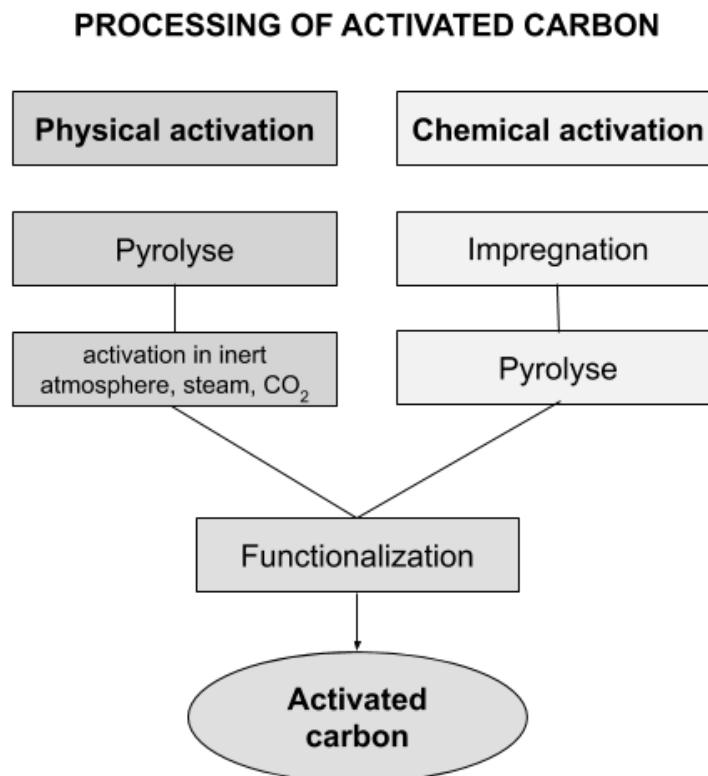


Figure 4: The different manufacturing processes to obtain activated carbon.



### 3. The different forms of activated carbon

Supplies of activated carbon can be found in several forms. The three most popular are the following ones [3]:

- the granular activated carbon (GAC), which has particles of different forms and their size vary between 0.2 and 5 mm,
- the powder activated carbon (PAC) where the particle's size is inferior to 0.18 mm;
- and the extruded activated carbon (EAC) where the activated carbon is extruded in a cylindrical shape with diameter from 0.8 to 5 mm.



Powder activated carbon      Granular activated carbon      Extruded activated carbon

Figure 5: the different forms of activated carbon. Figure adapted from [9].

### 4. Market of activated carbon

In 2015, the market of activated carbon was a US\$ 4.74 billion market and the estimation for 2021 is to reach US\$ 8.13 billion. This market growth is attributed to the recent environmental regulations, such as the control of mercury emission in the United States (Environmental Protection Agency) and regulations on water treatment but also to the development of new products [10]. What's more, activated carbon has been recently included in many formulas for beauty products and tooth path.

The main actors of this market are located in the US with Calgon Carbon Corporation, Cabot Corporation and Oxbow Activated Carbon LLC, in the Japan with Osaka Gas Co. Ltd, Kuraray Chemical Co. Ltd and KUREHA CORPORATION, in Germany with Donau Carbon GmbH and Silcarbon Aktivkohle GmbH and finally in the Sri-Lanka with Haycarb Plc. There are many other countries producing activated carbon such as France and China for example but in fewer quantities [10].



## B. Black liquor

### 1. Characteristics

The black liquor is a dense, dark liquid that is a by-product of the Kraft process used for the production of paper. In this process, wood is transformed into pulp removing the lignin and other undesirable components from the cellulose fibers.

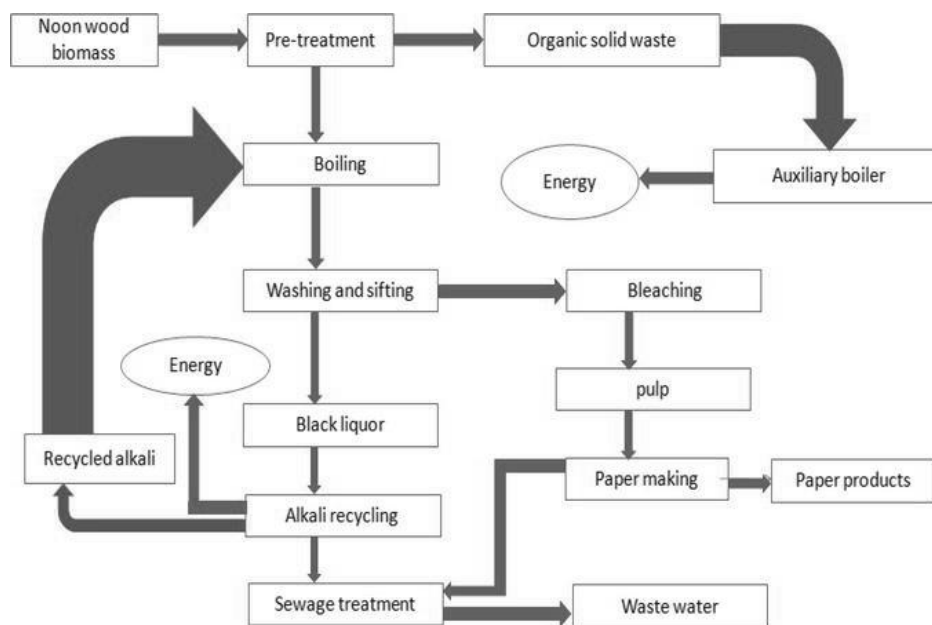


Figure 6: Papermaking process flowchart. Adapted from [11].

Then, these fibers are dried to make paper. Consequently, black liquor is mainly composed by lignin, hemicellulose and inorganic chemicals used in the process. The black liquor is extremely basic as it has a pH about 12,5 due to the alkaline conditions of the process [7]. Therefore, it can't be throwing out in the nature without treatment.

organic compounds	percent of dry solid
lignin	37.5
hemicellulose (saccharide acid)	22.6
carbohydrates (aliphatic acids)	14.4
fat and resinous acids	0.5



cellulose/ hemicellulose (polysaccharides)	3.0
<b>inorganic compounds</b> (NaOH, NaHS, Na <sub>2</sub> CO <sub>3</sub> , Na <sub>2</sub> SO <sub>4</sub> ...)	22
<b>TOTAL</b>	100

Table 1: A possible composition of black liquor. Adapted from [12].

## 2. Principal uses

Nowadays, black liquor is mainly used as fuel, lubricant or resin raw material. Actually, as the lignin has a calorific power about 26.6kJ/kg [7], the proper industry of paper uses it to generate energy in order to purify it or to treat it. Although, thanks to its carbonaceous nature, it has been revealed that it is also possible to produce activated carbon from pure black liquor without extracting lignin [7].

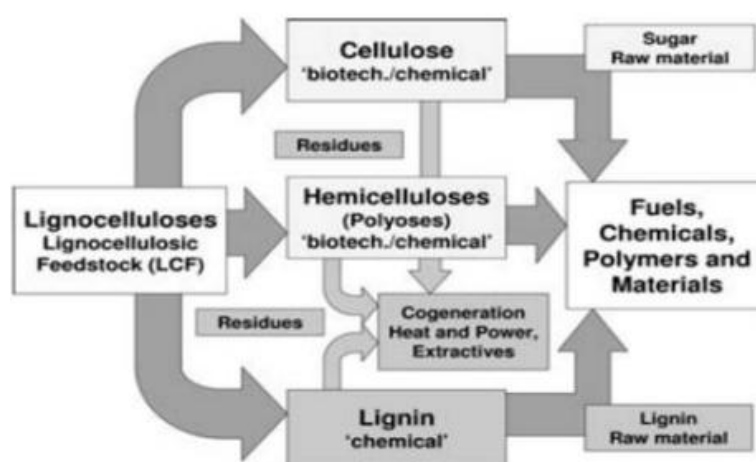


Figure 7: Synthetic view of the application of the lignocellulosic feedstock. Adapted from [13], copyright WILEY-VCH Verlag GmbH & Co. KGaA, Weinheim.

## 3. Biomedical properties of lignocellulosic materials

The main component of black liquor is lignin and it has been proved that after extraction, the lignin can show antioxidant and antibacterial properties [13]. With its phenolic hydroxyl and phenolic methoxy groups, some studies showed that lignin could be used to stabilize food which evidence antioxidant, antifungal and antiparasitic properties. Moreover, lignin has potential for applications in biomaterials. Consequently, some lignocellulosic raw materials have been recently used in biomedical applications for drug release or antibacterial uses and, like in our study



case, for tissue engineering throughout the manufacture of carbonaceous scaffolds [13-14].

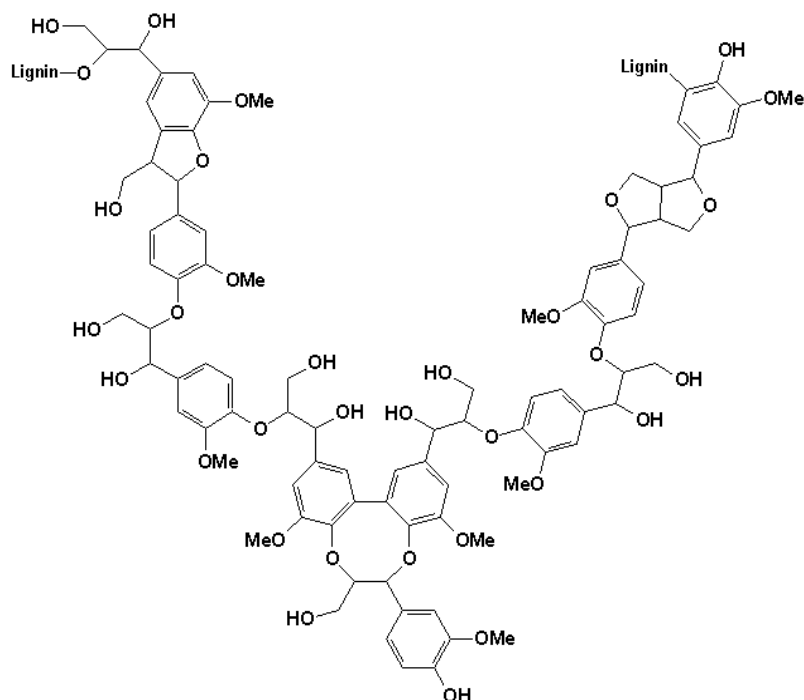


Figure 8: Chemical representation of a possible structure of a lignin. Adapted from [6].

#### 4. Market of black liquor and lignin

The world's cellulose production is actually around 500 million tons per year [7]. Most of this production, is it to say 90% of it, is produced by the Kraft pulping process [7]. During this process, for each ton of produced cellulose, it is generated one ton of black liquor residue [7]. Consequently, we can say that approximately 450 million tons of black liquor are produced per year. We can see that there is a huge opportunity on this cellulose by-product market. The derived products of lignin seem to be a good investment as market analysis from 2018 predicted that the global lignin market will have an annual growth of 2% until 2023 [13]. Many researchers are already working in this sector actually. In this project, the purpose is to use the pure black liquor as a raw material for activated carbon, one of the most valued materials in environmental challenges in addition to many other applications.



## C. Nanosilver particles

### 1. Characteristics

Silver, also known by the chemical symbol Ag, is the 47<sup>th</sup> element of the periodic table. Silver nanoparticles, Ag-NPs, are part of the family of nanoparticles, so basically, they are composed of metallic silver atoms, but the size of the resulting particles have dimensions ranged 1-100 nm [15-16]. When the particles reach the nanoscale, it can be observed that the properties of the material are way different compared to their bulk counterpart [17]. Due to the elevated ratio surface-to-volume, the interaction with the matter, including physical, chemical and biological properties, changes [15-17]. Thanks to these properties, silver nanoparticles have many applications in microelectronic, medicine, engineering, environmental science [11,17-18] just to cite few examples. That's why nanoscience has been one the favourite research areas ultimately [19].

### 2. Manufacturing process

In order to prepare Ag-NPs, there are four conventional processes: the chemical, the physical and the biological reduction and also the electrochemical route [15, 20].

The chemical reduction involves a metal precursor like silver salt which first is dissolved in a liquid in order to react with the reducing agent. Citrate, glucose, sodium borohydride or ethylene glycol are common agent in order to do the reduction. Then, to make the dispersion easier a stabilizing agent is used. The reduction of the silver salts involves nucleation and growing stages.

The physical reduction method uses silver which is reduced to Ag-NPs using radiations as a reductor agent. Some conventional physical methods use optical quantum reduction, microwave reduction, spark discharging and pyrolysis.

The biological reduction also uses silver ions, but this time instead of using a chemical method, bio-organisms are the ones who reduce ions to Ag-NPs. For this biological reduction, several bacteria's have been used including *Pseudomonas stutzeri* AG259, *Lactobacillus* strains, *Bacillus licheniformis* and *Escherichia coli*



(E.Coli) to cite some of them. Controlling the parameters of these reductions, the characteristics of the Ag-NPs can be tuned as desired.

The electrochemical synthesis is performed with a two electrodes-cell and a potentiostat or galvanostat. The cathode is generally composed of platinum or aluminium and the anode is composed of silver, generally a silver sheet [20-22]. The media need to contain a supporting electrolyte and a stabilizer to avoid agglomeration of silver nanoparticles. It has been proven that tetrabutylammonium bromide or acetate can be used as a supporting electrolyte and as a stabilizer [20-21]. The current density, or applied potential, is chosen depending on the desired size of nanoparticles but it always has to be close to the thermodynamic equilibrium to avoid the formation of irregular aggregates [20].

Synthesis of silver nanoparticles		
Method	Advantages	Disadvantages
<b>Chemical</b>	<ul style="list-style-type: none"> <li>- high yield</li> <li>- easy to produce</li> <li>- low cost</li> </ul>	<ul style="list-style-type: none"> <li>- use of toxic and hazardous agents</li> <li>- low purity</li> <li>- surfaces sedimented with chemicals</li> <li>- no well-defined size</li> </ul>
<b>Physical</b>	<ul style="list-style-type: none"> <li>- fast</li> <li>- no hazardous chemicals involved</li> <li>- radiations used as reducing agents</li> </ul>	<ul style="list-style-type: none"> <li>- high energy consumption</li> <li>- solvent contamination</li> <li>- no uniform distribution</li> <li>- low yield</li> <li>- very expensive</li> </ul>
<b>Biological</b>	<ul style="list-style-type: none"> <li>- environmentally friendly</li> <li>- high yield</li> <li>- defined size and shape</li> </ul>	<ul style="list-style-type: none"> <li>- depends on enzymes secreted by the bacteria</li> </ul>
<b>Electrochemical</b>	<ul style="list-style-type: none"> <li>- high purity</li> <li>- precise particle size control</li> </ul>	<ul style="list-style-type: none"> <li>- silver deposition occurs at the same time</li> </ul>

Table 2: Comparison between the different methods for the synthesis of Ag-NPs.

### 3. Antibacterial mechanism

The antibacterial effect is a result of the cytotoxicity of the Ag-NPs. Cytotoxicity is defined as the property to be toxic to cells is it to say to lead to cell's death. This cytotoxicity is intimately related to the size of the nanoparticle, size distribution, surface chemistry, particle morphology, particle composition, distribution rate,



agglomeration state, particle reactivity in solution, efficiency of ion release, cell type and reducing agent used for the synthesis. [17,19,23-24]. For example, some experiments [23] show that particle's size has an impact on cytotoxicity as it changes the surface area and consequently the surface reactivity: the smaller the Ag-NPs are, the higher the antibacterial activity is [19].

Until now, the antibacterial mechanism is not clear [17,19,23,25] yet but many observations have lead to some hypotheses about how the Ag-NPs can lead to cell-death.

First of all, in order to interact with human body, the Ag-NPs can be introduced in the organism by many pathways: through dermal contact, inhalation, intravenous injection, oral administration (passing by the gastrointestinal system), scaffold engineering... etc. After being introduced in the body, the Ag-NPs need to reach the inside of the bacteria's cells through cell membrane receptor recognition and internalization.

According to the researches [19, 23-25], once internalized, the Ag-NPs can induce cell death through various mechanisms at the same time. Some studies proved that the incoming of silver nanoparticles results in the excessive production of reactive oxygen species by the mitochondria which induce an oxidative stress and promote antibacterial mechanism [16-17,19,23]. The antibacterial mechanism is a consequence of the presence of silver ions inside the cell and of the oxidative stress generated. This antibacterial mechanism is characterized by various processes like: the inhibition of DNAase which leads to DNA damage [11, 18-19, 23]; the reaction between silver ions and the protons of the membrane eliminating the proton motive force, leading to membrane deficiency and therefore to the leakage of cellular material for growth [11,17,23]; the inactivation of enzymes by complexation with silver ions [11,17-18, 25], the activation of cell death-regulating pathways [19] and the attack of silver ions over the respiratory chain leading to mitochondrial and cell division deficiency [11,17,19].



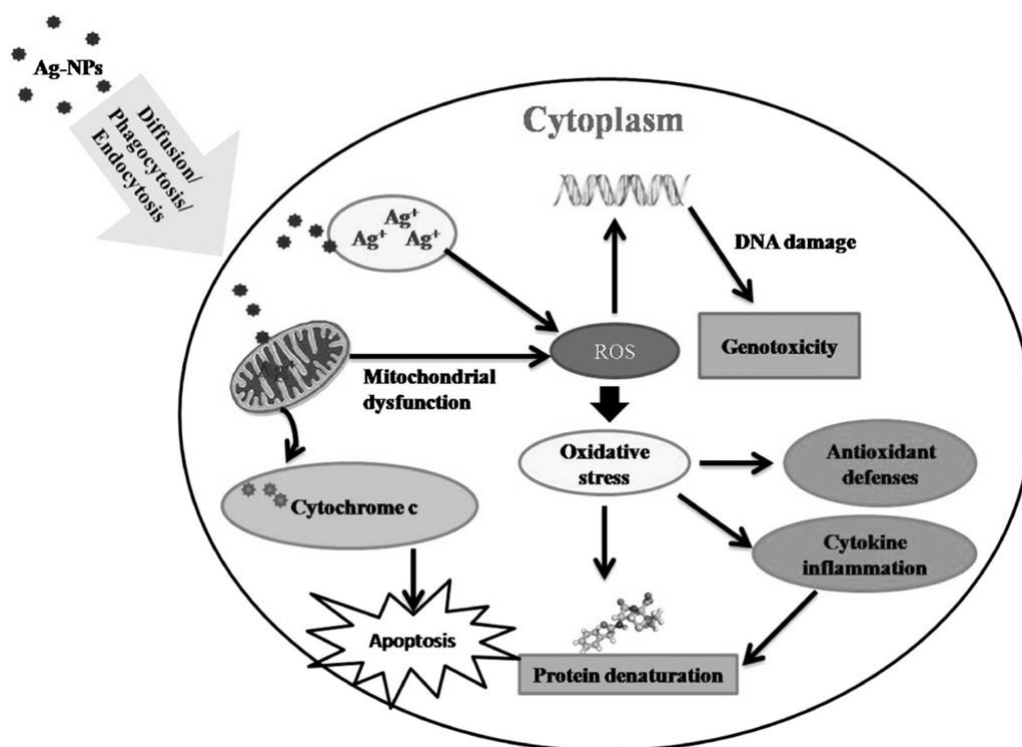
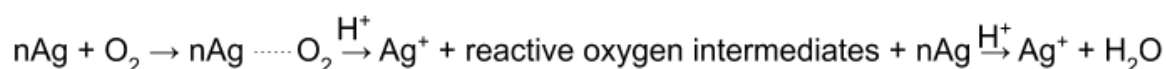


Figure 9: Possible uptake process and cytotoxic mechanism induced by silver nanoparticles. Adapted from [19].

#### 4. Silver nanoparticles and drug delivery

Nanoparticles, thanks to their size, have the potential to cross many biological barriers inside the body like blood barrier and cell membrane between others [26]. That's one of the reasons why recently, the use of nanotechnology in medicine has been a real focus for the research.

Known for their antibacterial properties, silver nanoparticles can be considered as a part of a drug delivery system as they contain active species, the silver ions which can be transported and delivered to a biological target [27]. The actual challenge about silver nanoparticles in biological media is to be able to control the release of silver ions. Recent studies have shown that most of the silver ions coming from AgNPs are generated by the oxidation process of the metallic silver particles by reacting with dissolved O<sub>2</sub> and protons in the media [27-29].



Equation 1: Principal mechanism for the release of silver ions from silver nanoparticles. Adapted from [27].



As oxidation is the main process for silver ions release, controlling the factors that influence oxidation, it could be possible to control silver ions delivery. Some of these factors are: the particle size of the silver nanoparticles, the oxidant availability, pre-oxidation treatment, the presence of sulphuric film or polymer coating and the media composition [27,29]. Some experiment show that ions release rate increases in the range of temperature of 0-37 °C [28] and decreases with increasing pH [28].

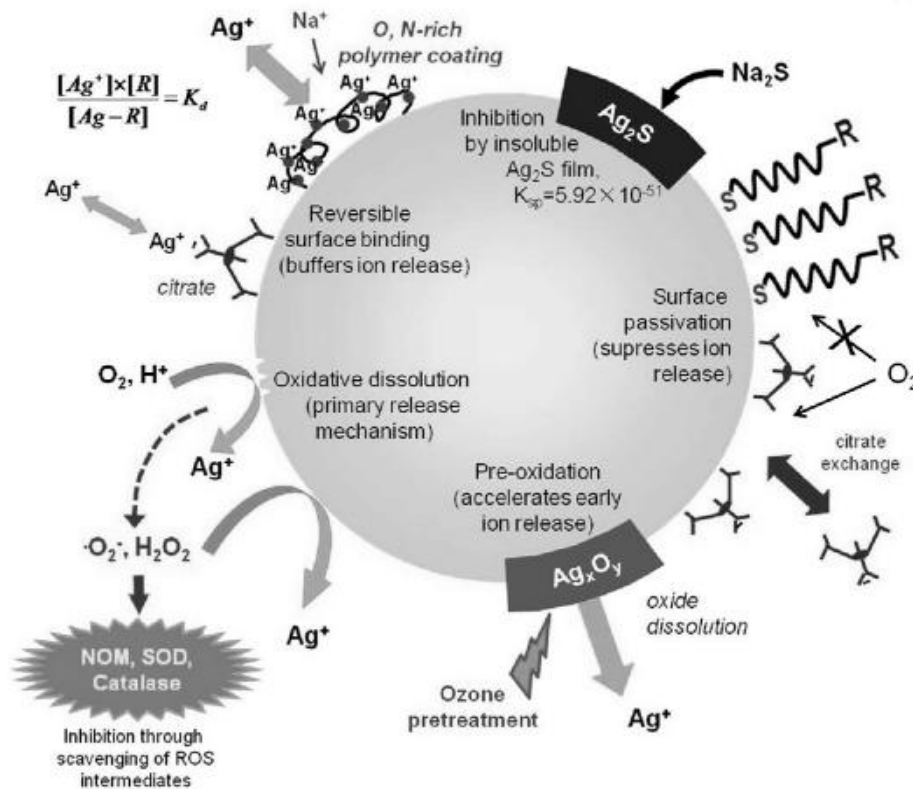


Figure 10: The different mechanisms that influence silver ions release. Adapted from [27].

## 5. Environmental, health and safety issues of silver nanoparticles

Nanoparticles have properties that are not shared with their bulk counterpart. First, they can be easily integrated by the organism through ingestion, respiration or dermal contact [30-31] and then, because of their huge ratio surface/volume, nanoparticles are found to be more reactive. In the literature [30], it can be found that in general, nanoparticles above 30 nm of diameter do not require regulatory scrutiny beyond that required for their bulk counterpart. Nevertheless, due to their enhanced reactivity, nanoparticles can generate ROS [17,30-31], which are involved in toxic



mechanisms, and can be oxidized which leads to the release of toxic ions in the organism [30-31].

Silver nanoparticles are said to have good antibacterial properties and low human toxicity for human cells [17], but information's about human and environmental health are lacking [31]. Specific studies on the toxicity of silver nanoparticles demonstrate that, even at a non-toxic dose, they are toxic for a variety of tissues including lung, liver, brain, vascular system and reproductive organs [31]. Consequently, there is a duality between antibacterial properties and toxicity.

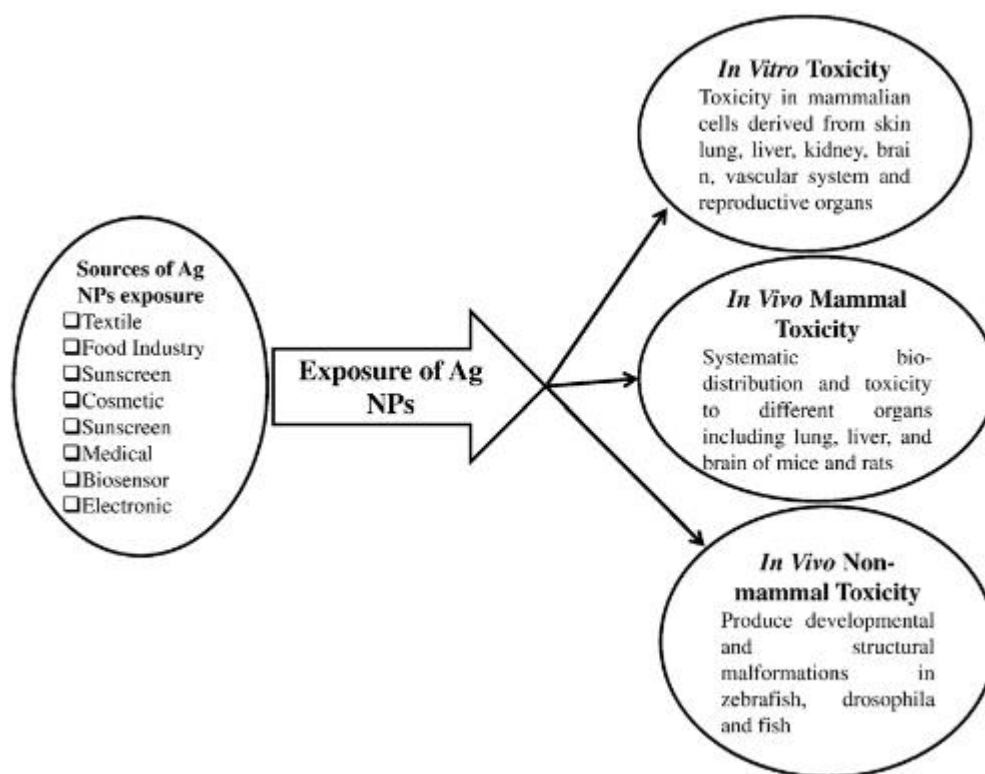


Figure 11: Sources of Ag NPs exposure and their adverse effects. Adapted from [31].

## 6. Principal uses

Silver nanoparticles in particular have been considered as one of the most interesting nanomaterial thanks to its effective antibacterial activity [16,19,23]. In daily life, people are surrounded by products containing silver nanoparticles: laundry detergent, room spray, water purification, toys, packaging materials but also in cloths as silver nanoparticles is used in the manufacture of socks and underwear. In medical area, silver nanoparticles are used in woundressind for burns and serious injuries, in surgical instruments and bone prosthesis to prevent infections [15-16,19].





Figure 12: Applications of silver nanoparticles. Adapted by the author.

#### D. Tissue engineering

During the last century, the traditional ways to cure organ and tissue damages were using one of the following methods: tissue grafting, organ transplantation or alloplastic and synthetic replacement. But these methods have some limitations. Tissue grafting and organ transplantation are limited by the number of donors and synthetic materials have difficulties to totally integrate with the host tissue and often fail after a certain period of time due to fatigue and adverse body response [32]. That's why since 1990, tissue engineering has been an active research area for regenerative medicine in order to solve the problems mentioned before [31-32]. Even if many biomaterials have been developed, biodegradable polymer that were already approved 30 years ago, are still the most employed. This fact highlights the complexity to translate new biomaterials to clinical practice [32]. Indeed, besides helping tissue regeneration, it is necessary to prove that the material is biocompatible, biodegradable and the degradation products have to be nontoxic and easily excreted by the metabolism [34].



## 1. Biomaterials used in tissue engineering

The principal materials used in tissue engineering are metals, ceramics, polymers and composites [35]. The metals are preferred when the scaffold need good mechanical properties for example in the field of bone regeneration. These metals are usually titanium, titanium alloys or stainless-steel [35]. For the ceramics, the calcium phosphate ones are preferred, thanks to their similar composition with human bone [34-35]. Inside the field of polymers, a huge diversity has been developed, synthetics or naturals. For the naturals, we find proteins as collagen and polysaccharide and for the synthetics, poly( $\alpha$ -hydroxy acid) and poly(glycolic acid) are usually used. But as their mechanical properties are reduced and their degradation is quick, composites, including bioceramics or bioactive glass, are investigated [34-36].

## 2. Regeneration process

Tissue morphogenesis is heavily impacted in presence of extracellular matrix (ECM) because of the interaction between ECM and cells. ECM like scaffold provides an architectural support for cell's development. Scaffolds are processed into 3D structures with determined characteristics of shape, size, architecture and physical properties; depending on the ones required in a specific application [37]. Generally, the ECM is also bioactive, which means that it has the capacity to interact with the biological environment in order to enhance the regeneration process [33]. It is important to consider the ECM as a dynamic matrix because its characteristics of composition and structure change along time as the degradation is happening [32-33]. Interconnected porous scaffold are well known for having a good shape to support cell growth and for having sufficient space to allow vascularization. Moreover, porous structures have a high absorbance capacity which is also favourable for cell adhesion and proliferation as it enhance water absorption, nutrient storage and nutrient exchanges [36].

### 1.1 Bone regeneration

After a critical size, the bone lesion is unable to regenerate which leads to nonunion. Massive lesion is consequently an huge challenge for reconstructive surgery [38]. Today, the common treatment is bone graft but the process is very risky



and painful [38]. That's why recently, biomaterial scaffolds have been used in surgery in order to promote migration, proliferation and differentiation of bone cells [32, 38]. In order to occur osteogenesis, it is important to have an appropriate porosity and porosity distribution for both cell and vascular invasions [32, 34, 38].

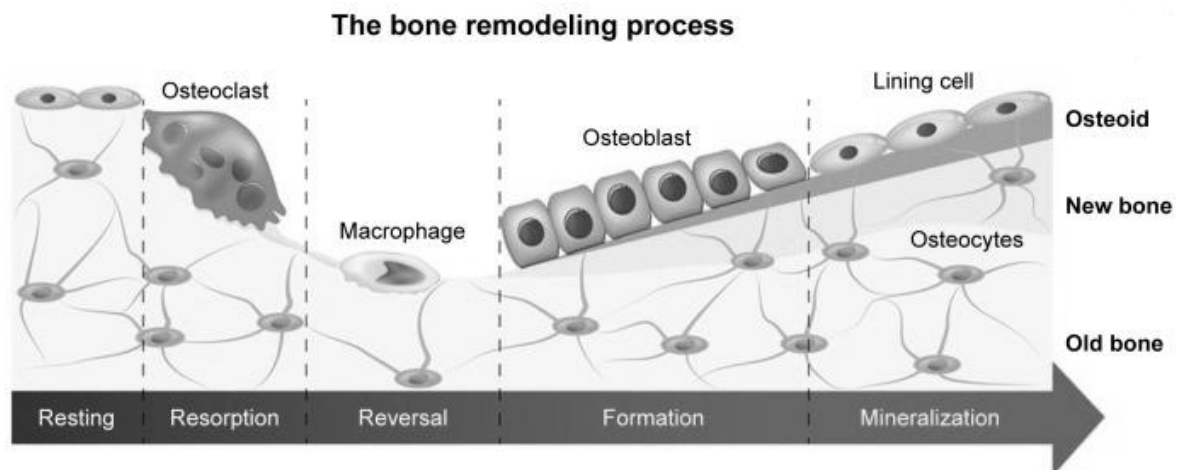


Figure 13: Scheme of bone regeneration process. Adapted from [39].

## E. Techniques of characterization

During all the steps of the project, it is essential to be able to characterize the produced materials to see if they fit the expectations or not. Many characterisation techniques allow to access composition, structural information, distribution, mechanical properties, concentration and many more. All the characterization techniques used during this study are going to be explained in the following paragraphs.

### 1. Scanning electron microscope (SEM) with Energy Dispersive X-Ray Spectroscopy (EDX)

SEM is a surface imaging method using an incident electron beam that scans the surface of the sample and interacts with it generating backscattered and secondary electrons. These electrons are detected in order to return a clear and high-resolution image of the samples surface. With these images, it is possible to evaluate texture and size of particles for example [40]. When the SEM is equipped with EDX, it is also possible to determine local composition in weight or atomic percentage. Indeed, EDX is frequently used to do qualitative analysis of composition [40].



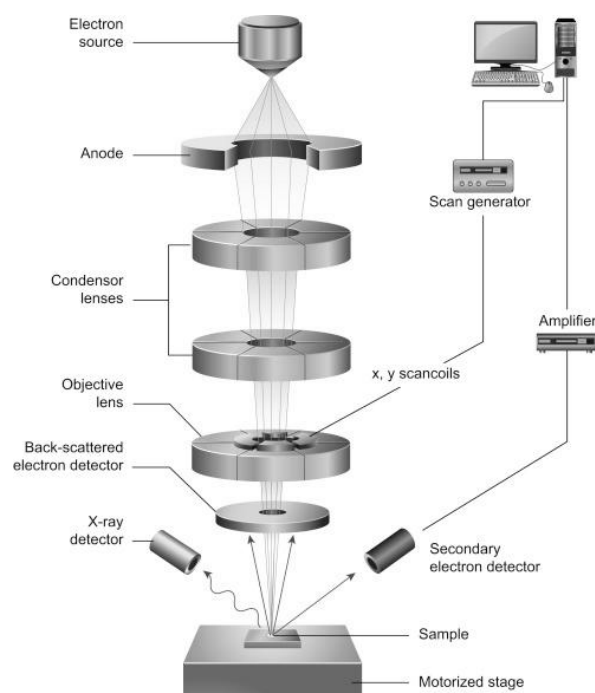


Figure 14: Structure of a SEM-EDX device. Adapted from [41].

## 2. Spectrophotometry

Spectrophotometry is a technique used to measure the absorbance of a chemical substance. The technique uses a beam of light that passes through the sample solution and interacts with it. Each chemical compound absorbs, transmits or reflects over a certain range of wavelength. So, it is possible to identify substances thanks to absorption spectrum. The spectrophotometer is the device that measures the intensity of light after it passes through the sample solution. If the chemical substance is known, it is also possible to access the concentration of the solution using the intensity detected [42].

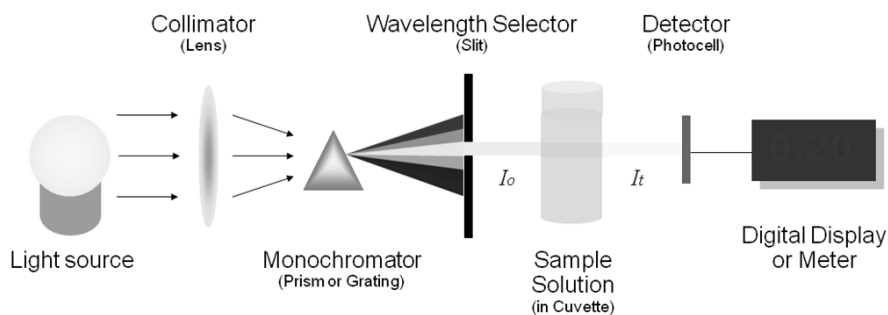


Figure 15: Basic structure of a spectrophotometer. Adapted from [42].



### 3. Dynamic light scattering (DLS)

The DLS method is used to determine the size of nanoparticles. These particles suffer Brownian motion as they are in suspension in a solution. Knowing the Stokes-Einstein equation, it can be seen that the speed of diffusion of this motion is inversely proportional to the diameter of the particle.

$$D = \frac{kT}{3\pi\eta d}$$

With :

D= diffusion coefficient

T= temperature (K)

$\eta$  = solvent viscosity

k = Boltzmann's constant

d = diameter of the particle

Equation 2: Stokes-Einstein equation. Adapted by the author.

In order to get particle's size, it is necessary to know the temperature and the solvent viscosity with precision. During the analysis, an incident light passes through the particle's solution and these particles scatter the light which create interferences (constructive or destructive). The intensity of the scattered light is then registered by a photomultiplier. The time dependency of the scattered light depends on the motion speed of the particles, and therefore on the particle size. Thanks to a digital correlator, it is then possible to know particles size from the analysis of scattered light [43-45].

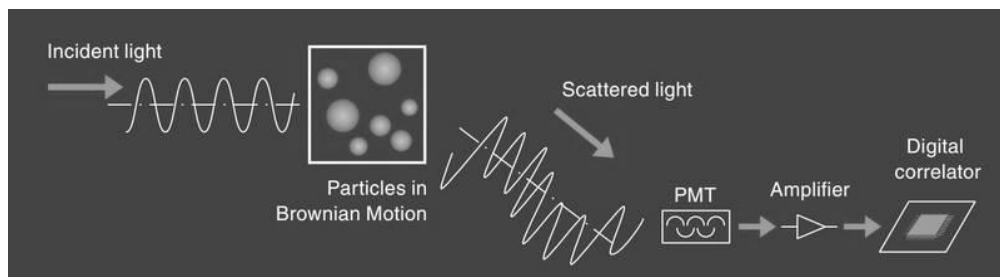


Figure 16: Basic structure of a DLS. Adapted from [43].



## II. Materials and methods

### A. Synthesis of activated carbon

#### 1. Polymerization of the material

The first step is to prepare the black liquor-based polymer. For that, pure black liquor was polymerised using formaldehyde. As a porous microstructure is required in order to allow cells to grow up inside the material, microscale polymethylmethacrylate (PMMA) is added. The PMMA is chosen because it is spherical which corresponds to the exigencies in terms of shape to create the porous structure.

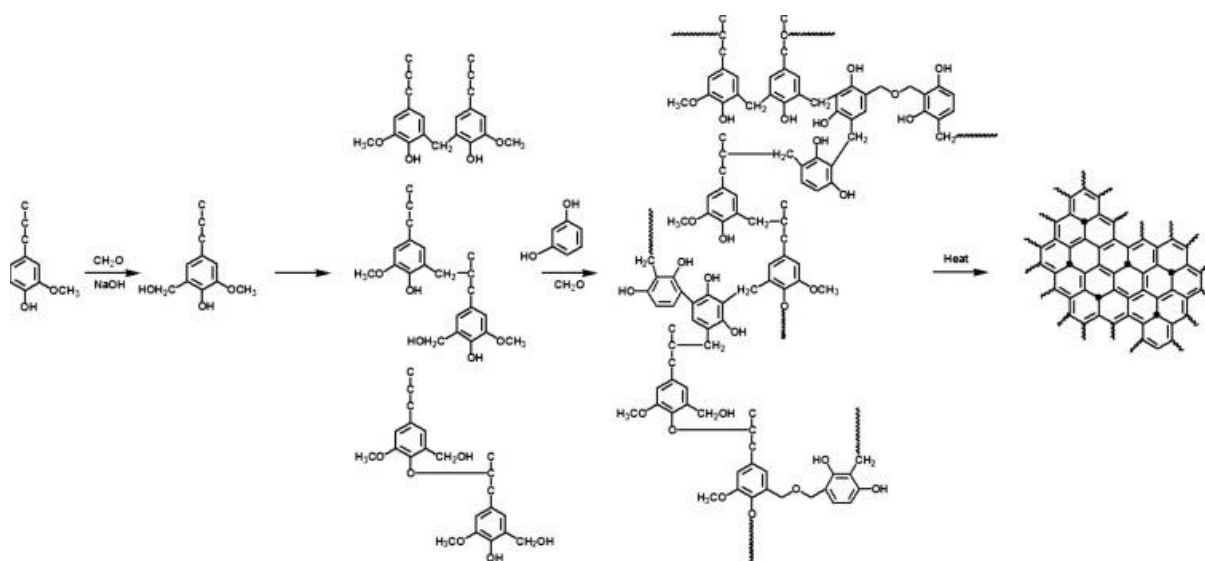


Figure 17: Reaction mechanism of lignin and resorcinol with formaldehyde under alkaline conditions. Adapted from [7].

### Materials

Reagents	Manufacturer/ Provider	Quantity
black liquor	SUZANO Papel e Celulose	100 g
PMMA ( Ø < 850 µm )	UNIGEL	45 g
Resorcinol (99-100.5%)	Synth® □	15 g
Formaldehyde (36.5-38%)	Synth® □	44 g

Table 3: List of reagents for the polymerization.





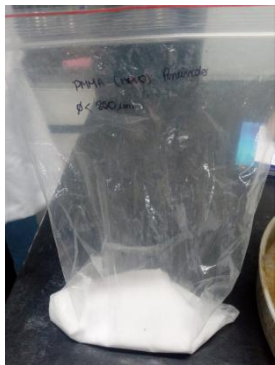

			
<b>resorcinol</b> <b>(C<sub>6</sub>H<sub>6</sub>O<sub>2</sub>)</b>  Synth® (100.5% of purity)	<b>formaldehyde</b> <b>(CH<sub>2</sub>O)</b>  Synth® (36.5-38% of purity)	<b>polymethyl- methacrylate</b> <b>(C<sub>5</sub>O<sub>2</sub>H<sub>8</sub>)<sub>n</sub></b>  provided by UNIGEL	<b>Black liquor</b> <b>(≈ 37.5 wt % of lignin)</b>  provided by SUZANO papel e celulose

Table 4: Materials used for the synthesis of the polymer.

## Process

After cleaning all the laboratory instruments, reagents are weighted in the following order :





(1)	(2)	(3)	(4)
			
Resorcinol	PMMA.	Black liquor	Formaldehyde

Table 5: Weight of the different reagents for the polymerization of black liquor.

Then, the magnetic bar is placed inside the becker of black liquor and the agitation system is turned on. Resorcinol is the first to be added. After it solubilizes entirely,



the PMMA is next added. The PMMA won't solubilize, it will stay in suspension inside the mixture, dispersed homogeneously. The last added is the formaldehyde.



Figure 18: Mixture of all the reagents for the polymerization.

The reaction starts and it is necessary to wait until it gets more viscous. To check this, it is possible to use a little spoon and stir the mixture to evaluate qualitatively the viscosity. When it starts to get really viscous, it is time to dump the mixture in the box.



Figure 19: Beginning of the polymerisation.

After this, it takes approximately one week for the reaction to end and for the formaldehyde to volatilize. It can be observed that at the end of the reaction, the material retracted.





Figure 20: Polymerized precursor of activated carbon.

Notes :

- Solid materials are weighted first because the black liquor can form a film on the surface without agitation and also, the formaldehyde volatilizes really quickly.
- It requires a special attention to observe when it gets more and more viscous in order to avoid solidification inside the becker.

Remarks (after adding the formaldehyde):

- 5 min: the becker started to get warmer.
- 20 min: the becker lower the temperature.
- 30 min: the mixture gets more viscous.
- 41 min: it reaches a good viscosity and it is time to dump the mixture in the box.
- 46 min: the mixture is solid inside the box.

## 2. Carbonization

In order to obtain a porous structure, it is required to pass by a carbonization step. During this step, all the materials, except the carbon skeleton, will volatilize. The places where the PMMA were located will form the porous.

During this step, the influence of the carbonization temperature and of the atmospheric gas inside the oven will be tested. In total, there are four different samples for four different conditions of carbonization.



Sample	Temperature (°C)	Furnace Atmosphere
1	1000	Argon
2	800	Argon
3	1000	CO <sub>2</sub>
4	800	CO <sub>2</sub>

Table 6: Carbonization conditions of the samples of activated carbon.

## Materials

- 1 alumina crucible
- 1 balance, AS2000C model with precision of two decimal places
- previously polymerized black liquor,
- 1 cylindrical oven, GRION Fornos Industriais, serial number 1731, year 2014.
- Argon 5.0 with purity of 99.9999%, provided by the society White Martins.
- CO<sub>2</sub> with purity of 99.99% provided by the society OXYLUMEN.

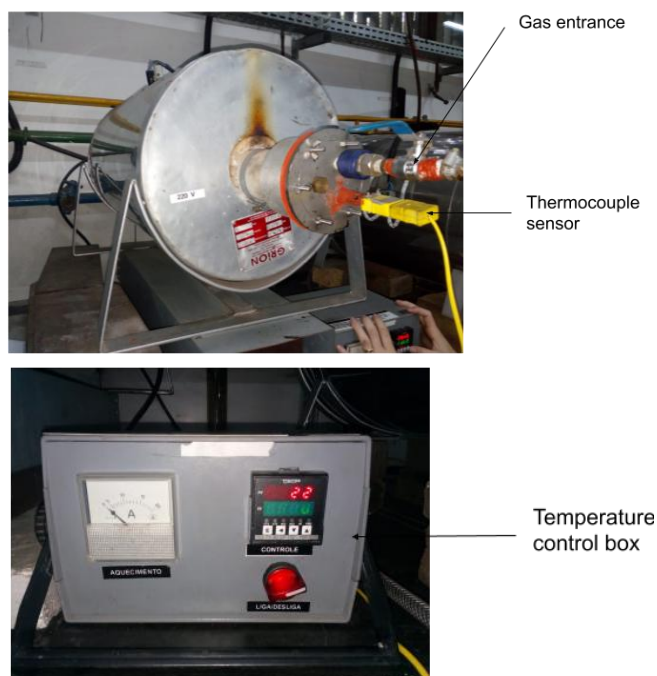


Figure 21: Descriptive scheme of the oven GRION Fornos Industriais.

## Process

The samples of polymerized material were cut, weighted (size sample around 20g) and inserted into the furnace over alumina crucible. The crucible is placed at the centre of the oven, where the temperature is known precisely thanks to the



thermocouple.

Depending of the temperature to be reached, the oven takes between 2-3 hours to warm-up with a ramp of 5 °C/min. Once the temperature stabilizes, it will remain at this temperature during 2 hours for the carbonization to occur. Then, it is necessary to wait until the temperature goes down to take off the sample.

As the sample carbonized at 1000 °C with CO<sub>2</sub> totally reacted, it has been necessary to change the procedure for the sample to carbonize at 800 °C with CO<sub>2</sub>: instead of flowing CO<sub>2</sub> during the entire process, argon has been used in the phases of heating and cooling. After the carbonization, the samples are weighted again to evaluate the carbon yield of the process.

Sample	Weigh (before carbonization)	Weigh (after carbonization)	Carbon yield
1	20.41 g	2.37 g	11.61%
2	20.24 g	5.17 g	25.55%
3	25.17 g	0 g	0%
4	25.36 g	1.54 g	6.07 %

Table 7: Weighs of the samples, before and after the carbonization.



Figure 22: Sample 1, a) before carbonization with argon at 1000 °C, b) after carbonization with argon at 1000 °C.



### 3. Washing

After the carbonization, only the carbon skeleton of the samples should stay. But in reality, some impurities coming from the composition of the black liquor remain. In order to remove the salts still present in the sample of activated carbon, it is necessary to pass by a washing step. A hand-made washing system including heating by return flow is used.

#### Materials

- water pump
- heater system
- volumetric flask of 2L
- ball condensator
- extractor (soxhlet)
- filter paper, 3 microns, 80g/m<sup>2</sup>
- tissue bags
- pumice stone
- distilled water

#### Process

Before washing, the samples have to be prepared. In order to have a minimal loss of materials during the washing, the samples have to be wrapped into filter paper. The filter paper will retain the fines particulates. It is necessary to put the samples wrapped in paper filter in the tissue bags.

To wash the samples, it is required to fulfil  $\frac{3}{4}$  of the volumetric flask with distilled water and put it in the heating system. Then, the protected samples can be inserted in the extractor (soxhlet). To be more efficient, it is possible to wet the samples adding distilled water in the extractor part. The extractor has to be properly fixed with the clamp and then the ball condensation device can be nested to the extractor. The all system needs to be plugged at 220V. It is important to verify the flow of the pump and check the heating system. Five entire days are necessary to complete the washing step.



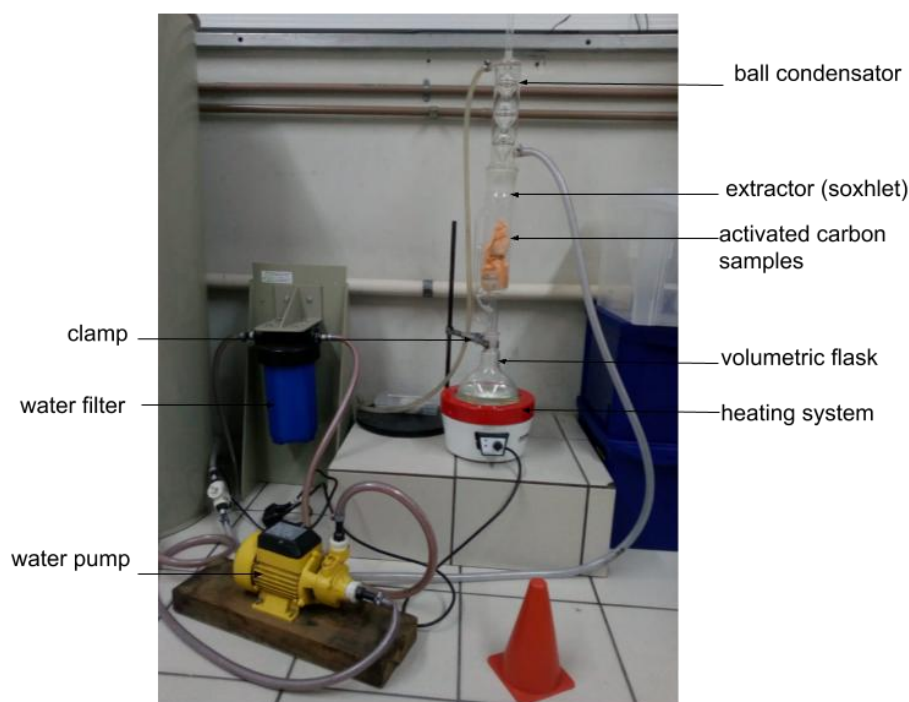


Figure 23: Description of the washing system.

#### 4. Drying

After the washing step it is necessary to dry the samples in order to remove the water.

##### Materials

- petri dishes
- 1 microprocessed oven for sterilization and drying, SPLABOR Equipamentos para laboratórios, SP400

##### Process

First, it is necessary to turn off the washing system and wait about 2 hours to cool down. Once done, the system is disassembled, and it is then possible to take out the samples. After opening the tissue bags, using the petri dishes, the samples (still wrapped into paper filter) are placed into the oven at a temperature of approximately 100 °C. If the pumice stone is still intact, it is possible to dry it to be able to reuse it in the future.





Figure 24: On the left, photograph of the oven used for the drying step. On the right (inside the oven), petri dishes containing the samples wrapped in filter paper.

## B. Impregnation with silver nanoparticles

### 1. Preparation of the solution of silver nanoparticles

In order to impregnate the material with silver nanoparticles, it is necessary to realize the synthesis of the silver nanoparticles solution. For the synthesis, the process described in the article [46] is used. It is important to know that the term of validity of the solution is about two weeks. After that, silver nanoparticles start to agglomerate, and it is no longer possible to use the solution for impregnation. Consequently, it is required to produce more than one solution during the period of the project.

## Materials

Reagents	Manufacturer / Provider	Quantity
solution of silver acetate (99%)	Dinâmica Química contemporânea	50 mL
solution of sodium borohydride (98%)	Êxodo científica	150 mL
polyvinyl alcohol (PVA)	Dinâmica Química contemporânea	5 drops

Table 8: Reagent used in the silver nanoparticle synthesis.



## Process

To prepare 200mL of silver nanoparticles solution following the instructions of the paper, it is required:

- 150mL of sodium borohydride solution with a concentration of  $2 \cdot 10^{-3}$  mol/L,
- 50mL of silver acetate solution with a concentration of  $10^{-3}$  mol/L.
- and 5 drops of solution of PVA 0.3%.

To prepare the PVA solution 0.3%, 0.3 g of solid PVA is mixed in 100 mL of distilled water. As the PVA is poorly soluble in water at environmental temperature, it is necessary to heat the PVA solution during 25 minutes in an oven at the temperature of 120 °C.

Knowing that the molecular weight of silver acetate is  $M=169.87$  g/mol and that the one of sodium borohydride is  $M=37.83$  g/mol it is possible to calculate the masses to weight:

- 0.0085 g of silver acetate
- 0.01135 g of sodium borohydride.

Once the theoretical part done, the analytic balance is used to weight our reagents:

Silver acetate	Sodium borohydride
0.0085 g	0.012 g

Table 9: Mass of reagents weighted to prepare the silver nanoparticles solution.

Then, the sodium borohydride is diluted with 150 mL of distilled water in the erlenmeyer and the silver acetate is diluted with 50 mL of distilled water in the becker. Right after the dilution, the solution of sodium borohydride needs to be placed in a bath of ice for 15 minutes. After waiting 15 minutes, the magnetic bar is added inside the erlenmeyer and it is placed on the agitation system. The next step is to add drop by drop (one drop per second) the silver acetate solution inside the cold sodium borohydride solution using eyedropper. The last step is to add 5 drops of the PVA solution recently prepared.





Figure 25: Solution of nanosilver particles.

Note : The PVA needs to be freshly prepared, if not the solution gets turbid.

## 2. Evaluation of the adsorption and desorption of silver nanoparticles by the samples of activated carbon

In order to investigate the adsorption and the possible desorption of silver nanoparticles by the samples of activated carbon along the time and in different environments several experiments have been realized. Our variables are: the concentration of the silver nanoparticles solution, pH (6.5, 7, 7.4) and temperature (37°C). As a matter of fact, the different pHs tested are aimed to simulate conditions of infection and inflammation (common reactions after bone surgery) as these reactions alter values of sanguine pH. This modification of pH can induce variation of the cell's permeability and lead to cell death. For the temperature, 37 °C corresponds to the regular body temperature. It is important to test if silver nanoparticles are liberated in these conditions.

	<b>Adsorption curves</b>	<b>Desorption curves</b>
Materials	Activated carbon samples + silver nanoparticles solution of 27 ppm	AC/AgNPs composites + physiological solution in different conditions
Procedure	Collects of solution after 15 min, 30min, 45min, 1h, 2h, 3h, 4h, 5h, 6h, 12h, 24h, 48h, 72h and 96h + Spectrophotometry	

Table 10: description of the experiment to obtain the adsorption and desorption curves.



### First experiment:

- **Solution:** H<sub>2</sub>O / H<sub>2</sub>O and fructose.
- **Samples:** activated carbon 800 °C / Ar and activated carbon 1000 °C / Ar.

This first experiment is to see if the impregnation of the activated carbon with silver nanoparticles could be done in simple solutions realizing a dilution of silver acetate in H<sub>2</sub>O and H<sub>2</sub>O + fructose media. In order to succeed, the first thing is to be capable to synthesize silver nanoparticles using this method. If it works, the adsorption of these silver nanoparticles by the samples of activated carbon is going to be monitored.

### Materials

Reagents	Manufacturer/ Provider	Quantity/ Concentration
Silver acetate (99%)	Dinâmica Química contemporânea	10 <sup>-3</sup> mol/L
Fructose (98%)	Synth ®	10% (mass)
Activated carbon (800 °C/Ar and 1000 °C/Ar)	produced in the laboratory	0.1g

Table 11: Reagents used in the first experiment.

### Process

The first thing to do is to grind the samples of activated carbon in order to obtain powder. Once this done, 20 mL of silver acetate solution can be added in each tube. To obtain a concentration of 10<sup>-3</sup> mol/L, it is required to weight 0.0033 g of silver acetate with the analytic balance for each tube and complete them with 20 mL of distilled water. In the case where there is fructose, it is added in a proportion of 10% of mass is it to say 2 g for each tube. It is necessary to stir the solution to solubilize the fructose. The last step is to weight and add 0.1g of activated carbon in each tube. As the silver is photosensitive, to avoid any kind of reaction with the silver nanoparticles, the tubes are covered with aluminium paper.



Reagents	Tube 1	Tube 2	Tube 4	Tube 5
silver acetate	0.0033 g	0.0033 g	0.0034 g	0.0033 g
fructose	2.008 g	2.0053 g	--	--
activated carbon	800 °C/Ar 0.1003 g	1000 °C/Ar 0.1004 g	800 °C/Ar 0.1002 g	1000 °C/Ar 0.1001 g

Table 12: Content of each tube for the first experiment.

Once the tubes are prepared, it is necessary to collect the samples of solution with a plastic eyedropper taking 1mL of the solution and keeping it in the plastic tube covered by aluminium paper for analysis. It is necessary to use a different eyedropper for each collect to avoid environmental contamination.

#### **Second experiment:**

- **Samples: activated carbon 800 °C/Ar, activated carbon 1000 °C/Ar and activated carbon 800 °C/CO<sub>2</sub>.**
- **To monitor adsorption: solution of AgNPs obtained by the process described above.**
- **To evaluate if there activated carbons liberate AgNPs: physiological solutions in different conditions.**

In this experiment, it is already known that there are silver nanoparticles in the solution, so it is possible to monitor the adsorption and desorption of the silver nanoparticles by the different samples of activated carbon.

#### **Materials**

- 1 microprocessed oven for sterilization and drying, SPLABOR Equipamentos para laboratórios, SP400
- 1 pHmeter GEHAKA, calibrated NBR ISO/IEC 17025

#### **Process**

In this case too, it is necessary to grind the activated carbon and weight it before adding the solution of silver nanoparticles for impregnation. The quantities of



activated carbon have been chosen in order to be able to do the different desorption's after. As for the previous experiment, it is required to cover the tubes with aluminium film. Then the collects of solution can be realized with the same time intervals as previously described in order to obtain the adsorption curves after spectrophotometry.

Reagents	Tubes 1,2,3,4	Tubes 5,6,7,8	Tubes 9,10,11,12
AgNp solution	20 mL	20 mL	20 mL
activated carbon	800°C/Ar 0.05 g	1000°C/Ar 0.05 g	800°C/ CO <sub>2</sub> 0.014 g

Table 13: Reagents used in the second experiment during the adsorption phase.

Once the adsorption is done, the samples are dried inside the oven at 100 °C. After that, the desorption phase can start.

To obtain solutions at different pHs, physiologic serum (pH 5.49) and a solution of sodium hydroxide have been used. It is necessary to add drop by drop the solution of sodium hydroxide 1 mol/L in the physiological serum in order to reach pH of 6.5, 7 and 7.4.

For the test with temperature, a water-bath with a controlled temperature at 37 °C was used.

	Tube 1	Tube 2	Tube 3	Tube 4
Impregnated activated carbon	800 °C/Ar 0.05 g	800 °C/Ar 0.05 g	800 °C/Ar 0.05 g	800 °C/Ar 0.05 g
pH	6.5	7	7.4	--
temperature (°C)	--	--	--	37

Table 14: Description of the desorption experiment for the activated carbon carbonized with argon at 800 °C.

	Tube 5	Tube 6	Tube 7	Tube 8
Impregnated activated carbon	1000°C/Ar 0.05 g	1000°C/Ar 0.05 g	1000°C/Ar 0.05 g	1000°C/Ar 0.05 g
pH	6.5	7	7.4	--
temperature (°C)	--	--	--	37



Table 15: Description of the desorption experiment for the activated carbon carbonized with argon at 1000 °C.

	Tube 9	Tube 10	Tube 11	Tube 12
Impregnated activated carbon	800 °C/ CO <sub>2</sub> 0.014 g	800 °C/ CO <sub>2</sub> 0.014 g	800 °C/ CO <sub>2</sub> 0.014 g	800 °C/ CO <sub>2</sub> 0.014 g
pH	6.5	7	7.4	--
temperature (°C)	--	--	--	37

Table 16: Description of the desorption experiment for the activated carbon carbonized with CO<sub>2</sub> at 800 °C.

Collects of solution are realized with the same time intervals as previously in order to obtain the desorption curves using spectrophotometry.

The samples of activated carbon are finally dried in the oven at 100°C.

### 3. Evaluation of the bactericidal activity

#### Materials

- phosphate buffer saline (PBS)
- brain heart infusion (BHI)
- polystyrene tissue culture plate with 96 cavities, KASVI

#### Process

In order to evaluate the bactericidal comportment of the samples against *E.Coli* (gram-negative bacteria), the solutions of silver nanoparticles and the impregnated samples of activated carbon were tested separately. Sterile culture plates were used for the tests. The bacteria was incubated during 24h before starting the experiment. Before preparing the tissue culture plate, it is necessary to irradiate all the materials used in the experiment with UV-light during 10-15 min in order to sterilize. Only the bacteria and the silver nanoparticles solutions are not irradiated. After sterilization, all the experiment needs to be done using a laminar flow cabinet and using gloves. The tissue culture plate was prepared as described in the figure



26. The evaluation of the quantity of bacteria was realized using a spectrophotometer. Lower is the absorbance; lower is the quantity of bacteria.

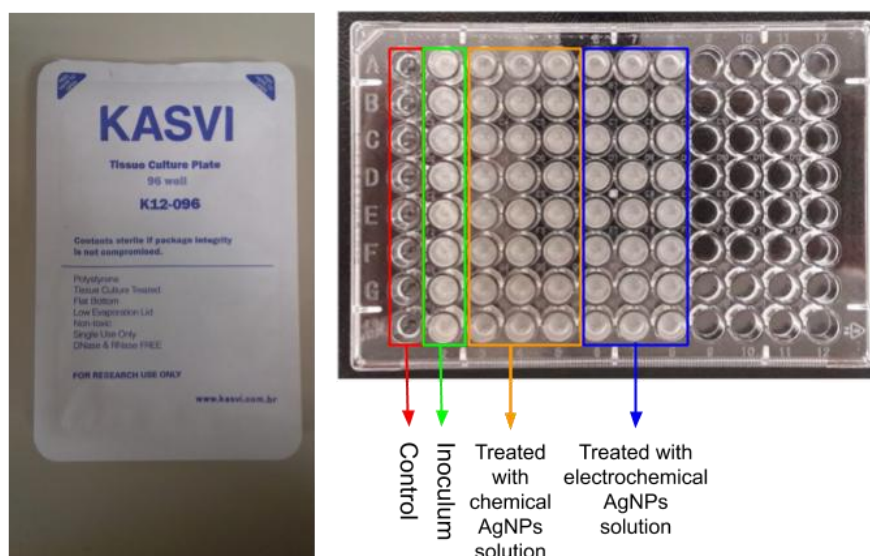


Figure 26: Organization of the the tissue culture plate used for the test of the AgNPs solution.

- The first column is the control one. It contains phosphate buffer and brain heart infusion. This column is the reference to know if contamination happened and therefore, if the results of the plate are usable. As this column doesn't contain bacteria, it has to be translucent.
- The second column is the inoculum. It contains phosphate buffer, BHI and *E.Coli* bacteria's. As this column doesn't contain treatment, bacteria's have to grow in order to trust the plate's results. As bacteria's grow, the solution becomes turbid.
- The other columns are used to test the treatment. They contain phosphate buffer, BHI, *E.Coli* bacteria's and the treatment to test.

First, the solution of AgNPs, prepared as described a few sections above, has been tested. Its concentration of AgNPs was about 27 ppm. As this concentration was really low, other solutions of AgNPs concentrated in 54 ppm and 81 ppm have been prepared (multiplying the quantities of reagents by 2 and 3 respectively) and tested on tissue culture plate.



Also, the different samples of activated carbon have been impregnated with these solutions of 27 ppm, 54 ppm and 81 ppm for 5 days, then dried in the oven at 100 °C and finally tested on tissue culture plate.

#### 4. Characterization techniques

All the SEM-EDX analyses were performed without overlying the samples and using the INSPECT F50 microscope model with an EDAX detector for EDX analysis provided by AMETEK Materials Analysis Division.

The DSL analysis was performed by a Zetasizer Vers.7.11 model provided by Malvern Instruments Ltd.

In the experiments realized to monitor adsorption and desorption of silver nanoparticles, the spectrophotometer SHIMATSU UV 1800 in a range of 300 nm - 800 nm was used to measure absorbance.

The lecture of the tissue culture plate was realized with a spectrophotometer ANTHOS 2020 with a wavelength of 590 nm .

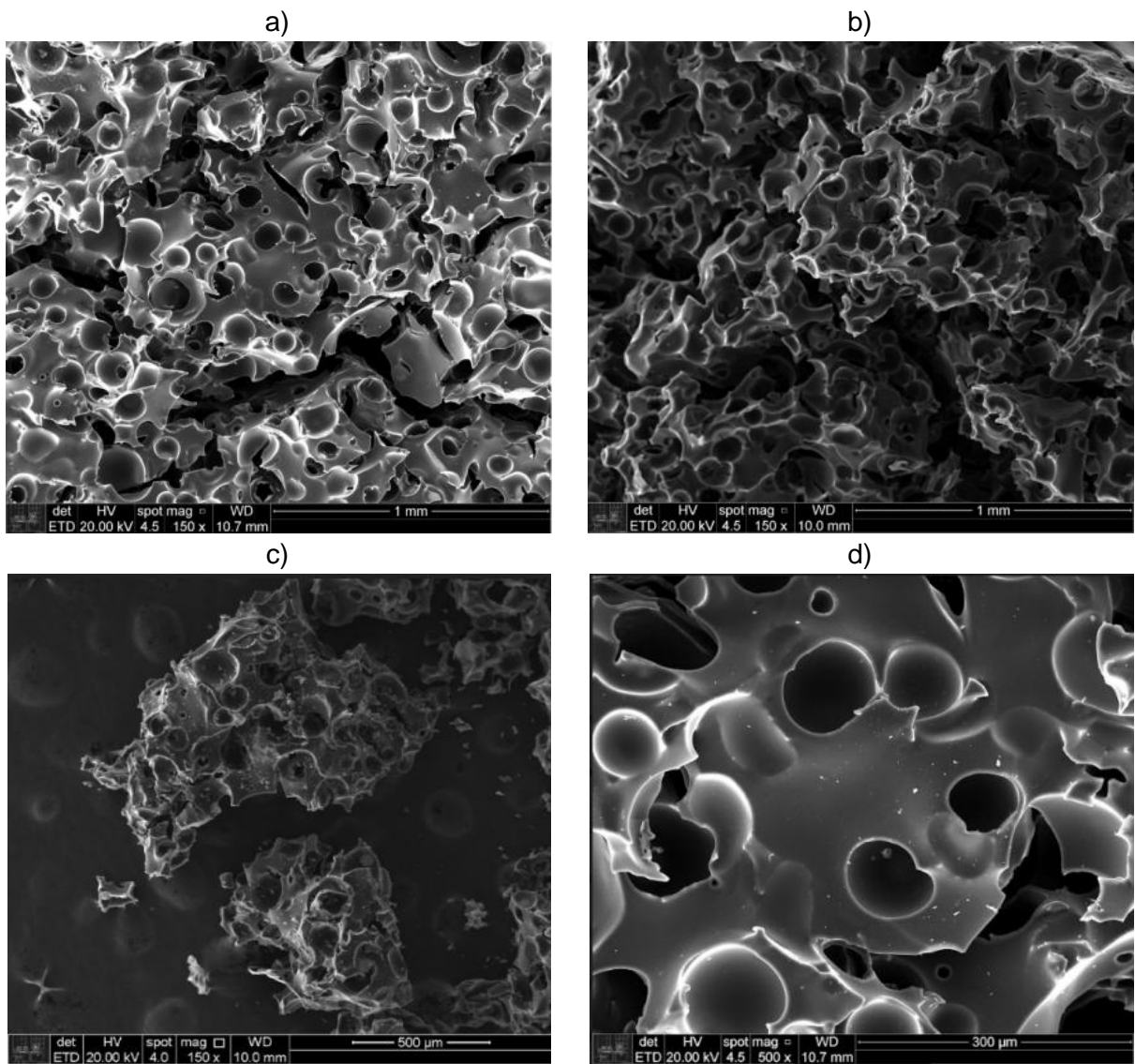


### III. Results

#### A. Activated carbon structure and composition in different conditions of carbonization

##### 1. Structure analysis

In order to evaluate the influence on activated carbon structure of both temperature and atmosphere used in during the carbonization, SEM microscopy has been used.





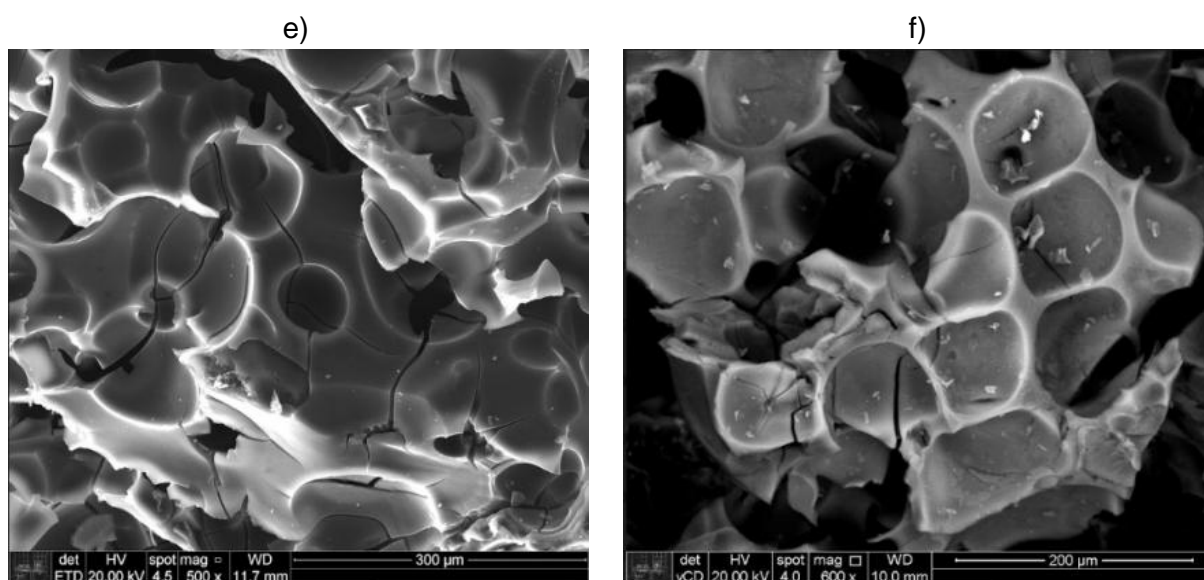


Figure 27: a) AC-Ar-800 °C, x150; b) AC-Ar-1000 °C, x150; c) AC-CO<sub>2</sub>-800 °C, x150; d) AC-Ar-800 °C, x500; e) AC-Ar-1000 °C, x600; f) AC-CO<sub>2</sub>-800 °C, x600.

SEM images show that an extremely porous structure was obtained independent of the conditions of the carbonization. It can be observed that on the sample carbonized with argon at 1000 °C, there are more cracks than on the sample carbonized with argon at 800 °C but both have a smooth surface. For the sample carbonized with CO<sub>2</sub> at 800 °C, cracks are also visible. Also, it presented a rough surface probably due to the CO<sub>2</sub> that interacts with the carbon of the sample and which leads to a higher loss of material. These characteristics suggest that the brittleness of the samples follow this order: AC-800 °C-CO<sub>2</sub> > AC-1000 °C-Ar > AC-800 °C-Ar.

It was possible to approximate pore diameter using the ruler of the SEM software.



### Average pore diameter ( $\Phi_m$ ) of the different samples of activated carbon

<p>AC carbonized with Ar at 800°C, magnification x500</p>	<p>AC carbonized with Ar at 1000°C, magnification x250</p>	<p>AC carbonized with CO<sub>2</sub> at 800°C, magnification x300</p>
$\Phi_m = 97.56 \mu\text{m}$	$\Phi_m = 125.47 \mu\text{m}$	$\Phi_m = 103.06 \mu\text{m}$

Table 17: Average pore diameter ( $\Phi_m$ ) of the different samples of activated carbon.

In all samples, it is visible that macroporous were obtained. Observing the photographed regions of the two samples carbonized with argon, it can be deduced that higher temperature leads to larger pores. Also, it can be suspected that using CO<sub>2</sub> atmosphere rather than inert atmosphere, larger pores are obtained. Even if the use SEM images isn't a precise technique to characterize pore size, it can be considered that these pictures are representative of the all samples as there were randomly chosen.

## 2. Composition analysis

In order to estimate the chemical composition of the samples of activated carbon, EDX analyses obtained with the SEM microscope were realized.

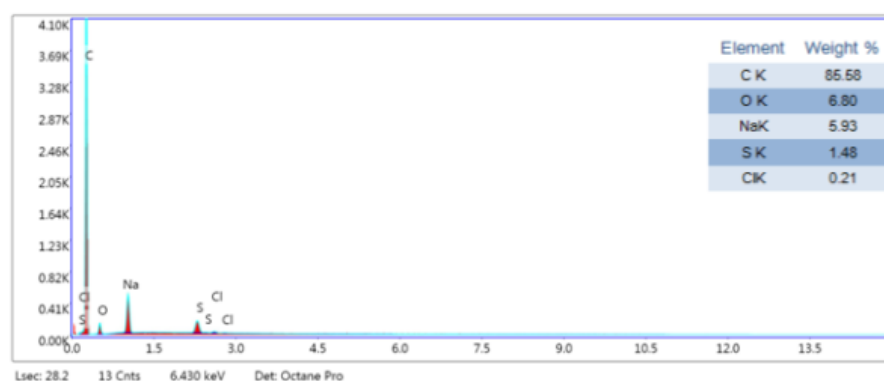


Figure 28: Composition of the sample of activated carbon, after carbonization with argon at 800 °C.



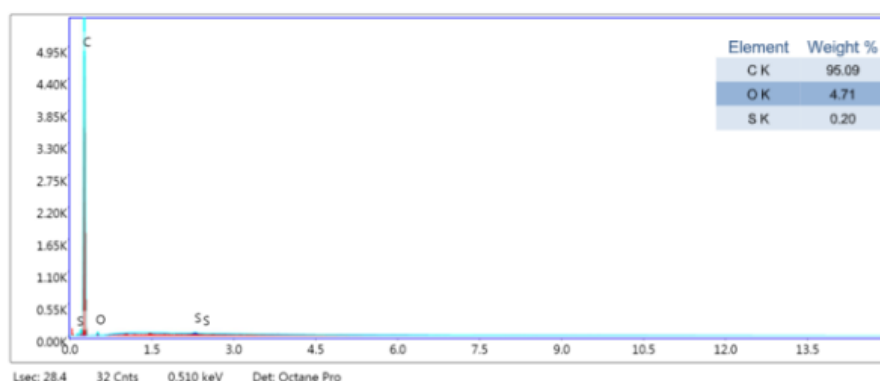


Figure 29: Composition of the sample of activated carbon, after carbonization with argon at 1000 °C.

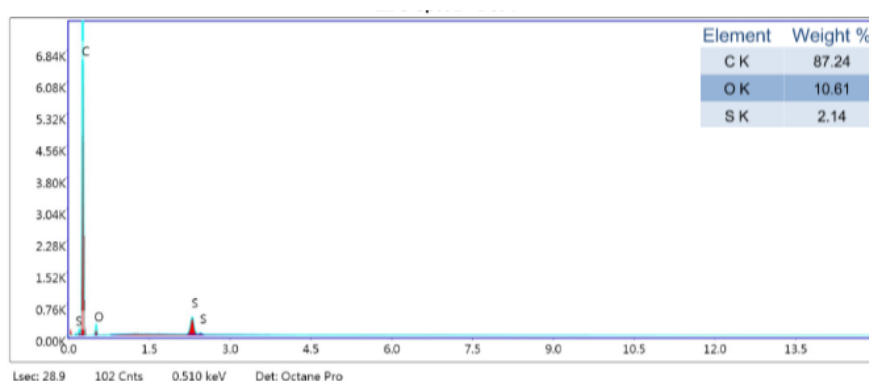


Figure 30: Composition of the sample of activated carbon, after carbonization with CO<sub>2</sub> at 800 °C.

In the EDX spectrum of the different samples of activated carbon, the presence of carbon, oxygen and sulphur with sodium and chlorine for the one carbonized at 800 °C with argon was observed. This corresponds to the expectation: in all the samples, the carbon skeleton remains and the PMMA volatilized. The sodium, sulphur and the chlorine come from the black liquor. It is evident that elevating temperature, more components volatilize, and the activated carbon is purer. Even if the EDX analysis is only semi-quantitative, the carbonizations with argon at 800 °C and the carbonization with CO<sub>2</sub> at 800 °C seem to lead to higher quantity of oxygen.

## B. Characterization of silver nanoparticles

### 1. Silver nanoparticles size distribution

The DLS analysis of the AgNPs solution is fundamental in order to find out the size distribution of the silver nanoparticles synthesized. The analysis of the AgNPs solution with a concentration of 27 ppm was performed.



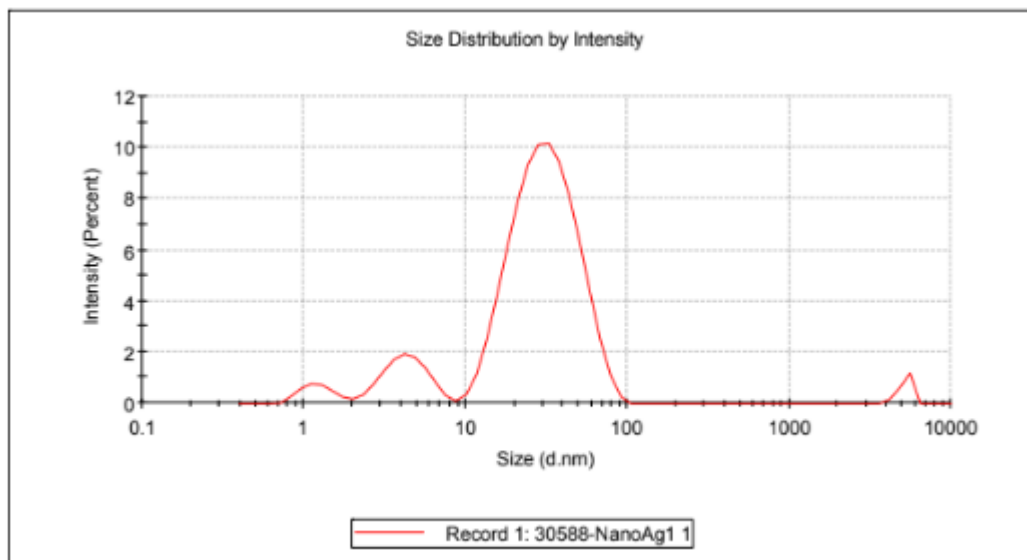


Figure 31: Size distribution of the silver nanoparticles in the solution 27 ppm concentrated.

	Size (d.nm):	% Intensity:
Peak 1:	33,41	83,9
Peak 2:	4,403	10,7
Peak 3:	1,259	3,4

Figure 32: Details of the size distribution of the silver nanoparticles.

Most of the synthesized nanoparticles have a diameter near 33 nm, in a range of 10-100 nm. Smaller particles were also synthesized, with a diameter in a range of 1-10 nm but in a low quantity.

## 2. Antibacterial activity of the silver nanoparticles solutions

### **Solution containing 27ppm of silver nanoparticles**

Using the processing previously described, the following tissue culture plate was divided as described below and analysed using spectrophotometry.



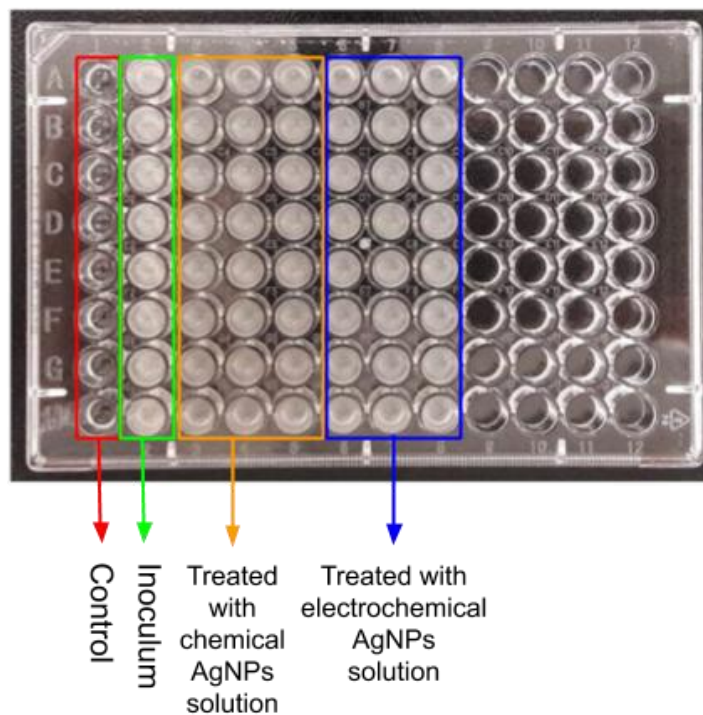


Figure 33: Tissue culture plate used to test the chemical AgNPs solution of 27ppm and its disposition.

	1	2	3	4	5	6	7	8	9	10	11	12
A	0,08	0,99	0,875	0,876	0,88	0,779	0,823	0,757				
B	0,09	0,86	0,714	0,75	0,78	0,712	0,7	0,753				
C	0,065	0,837	0,742	0,805	0,771	0,721	0,676	0,758				
D	0,067	0,802	0,742	0,701	0,708	0,663	0,682	0,713				
E	0,062	0,775	0,691	0,726	0,701	0,671	0,703	0,702				
F	0,086	0,809	0,646	0,668	0,661	0,621	0,62	0,613				
G	0,075	0,833	0,588	0,65	0,613	0,591	0,561	0,609				
H	0,0123	0,816	0,56	0,598	0,607	0,58	0,606	0,565				

Figure 34: Results of the analysis given by the spectrophotometer.

By doing a simple observation, it is clear that there is a reduction of the bacteria's growth in the cavities where the AgNPs solution has been used as the cavity is less turbid than the inoculum. For the one synthesized by chemical route, there is an average reduction of bacteria of 15.4% with standard deviation of 0.09. This reduction could seem small but in fact, the concentration of AgNPs in the solution is very low (27ppm only) and these results are encouraging. In order to see if higher concentration gets better bactericidal results, the experiment has been repeated with concentrations of 54ppm and 81ppm.



The results for the AgNPs synthesized by electro-chemical route won't be discussed here as they aren't part of this project.

### Comparison of the bactericidal efficiency of the solution containing 27ppm, 54ppm and 81ppm of silver nanoparticles

Using the same method, bactericidal analyses have been realized for solutions with 54ppm and 81ppm of AgNPs. Following, the tissue culture plate used and its disposition.

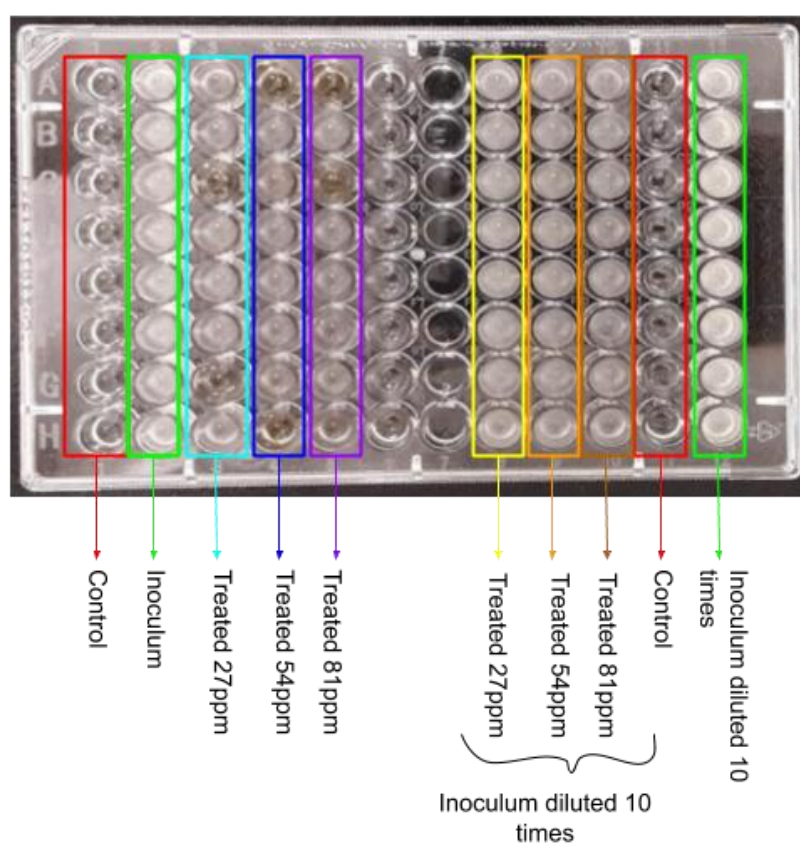


Figure 35: Tissue culture plate used to test AgNPs solutions of 27ppm / 54ppm / 81ppm and its disposition.

	1	2	3	4	5	6	7	8	9	10	11	12
A	0,063	0,839	0,586	0,091	0,099			0,801	0,82	0,815		0,801
B	0,057	0,796	0,566	0,531	0,629			0,722	0,719	0,755		0,849
C	0,056	0,739	0,068	0,39	0,096			0,742	0,705	0,696		0,886
D	0,057	0,803	0,535	0,48	0,457			0,7	0,718	0,583		0,832
E	0,061	0,777	0,575	0,5	0,436			0,711	0,753	0,571		0,833
F	0,057	0,812	0,476	0,421	0,322			0,668	0,632	0,423		0,817
G	0,056	0,608	0,071	0,385	0,452			0,557	0,608	0,598		0,797
H	0,065	0,666	0,446	0,09	0,239			0,499	0,581	0,518		0,785



Figure 36: Results of the analysis given by the spectrophotometer.

It is visible by eye observation that this time, the antibacterial activity is higher and, in some cavities,, the solution is translucent which means that there is no bacteria grew. Indeed, for these cavities, the absorbance is really weak (highlighted in red on the picture). The average reductions for the three concentrations tested are resumed in the following graph:

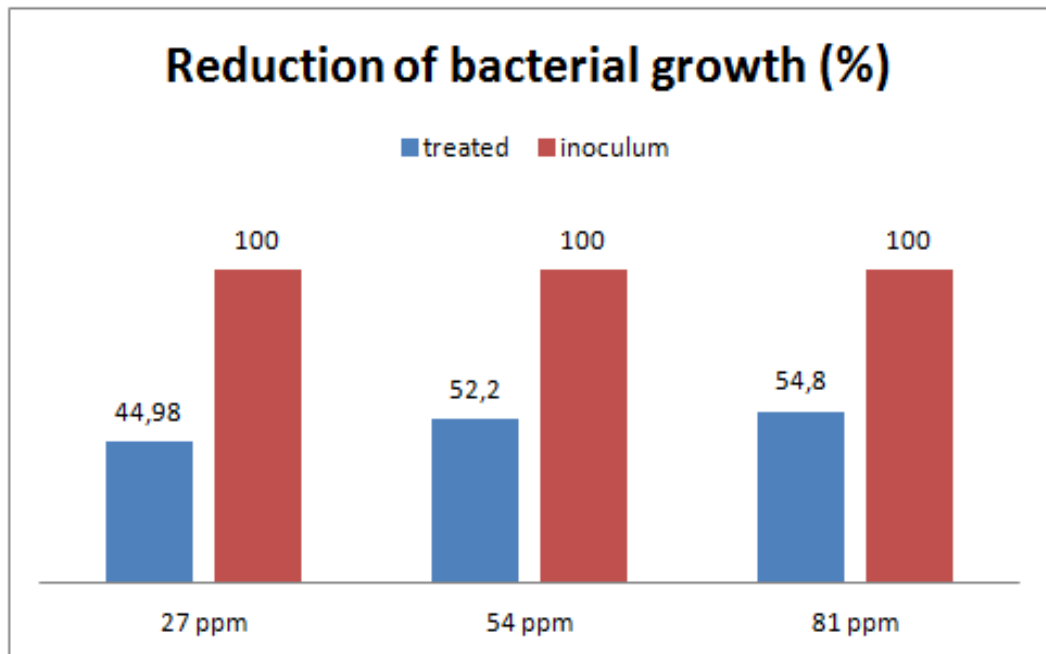


Figure 37: Average reduction of bacterial growth treating with AgNPs solutions of 27 ppm, 54 ppm and 81 ppm.

It is clear that increasing the concentration, the efficiency against bacteria's growth increases too. The most efficient was the solution with 81ppm of silver nanoparticles which reaches almost 55% of average reduction of bacterial growth. It is important to remember that in this case, observing the results one by one, some tests proved a radical reduction. In these tests (results highlighted in red), the average reduction of bacterial growth is about 88%. For now, it is impossible to explain the isolation of these results (it can be due to an abnormal dump of the inoculum for example) so it will be necessary to repeat the experiment. Also, in this experiment, the efficiency of the 27ppm solution of AgNPS was really different from the first experiment where the reduction of bacterial growth reached 15% only. As the same solution was used one week after, it is possible that the particles agglomerated and that the particle size



influences the efficiency. The experiment will be renewed with freshly prepared solution in order to verify this point.

On the tissue culture plate, the antibacterial activity of the solutions was also tested with inoculums diluted 10 times in order to see if the concentration of bacteria has an effect over the bactericidal efficiency of the silver nanoparticles solutions. Average bacterial growth reductions are about 18.2%, 16.1% et 24.9 wt.% for the solutions of 27 ppm, 54 ppm and 81 ppm respectively. These results aren't better than the ones obtained with the inoculum without dilution which highlights the fact that bacterial growth is controlled by the bacteria metabolism and doesn't depend on bacterial concentration.

### C. Analysis over the composite of activated carbon and silver nanoparticles

#### 1. Analysis of the silver nanoparticles adsorption by activated carbon samples using spectrophotometry

As described in the section materials and method, the adsorption of silver nanoparticles by the activated carbon samples has been monitored collecting samples of solution periodically and analysing them with a spectrophotometer.

For the test using fructose (first experiment), the absorbance was always null which means that silver nanoparticles weren't synthesised. Therefore, null absorbance was monitored.

For the second experiment, the peak of absorbance is always observed for a wavelength in a range of 400 nm - 450 nm which corresponds to the region of absorption of silver nanoparticles [47]. The peak isn't encountered always at the same wavelength because it depends on the silver nanoparticles size. As it has been determined with DLS analysis, the silver nanoparticles contained in the solution of 27ppm follow a distribution size, so the results are coherent.



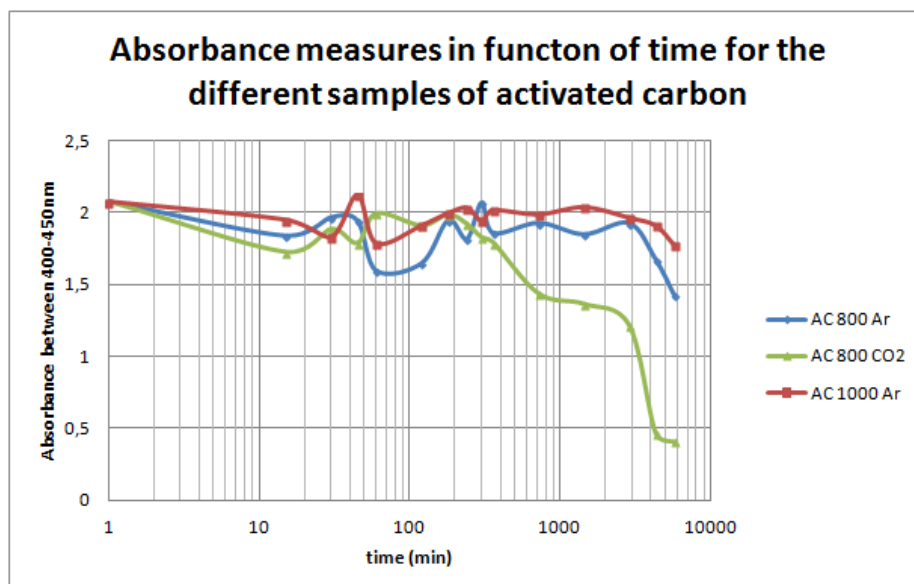


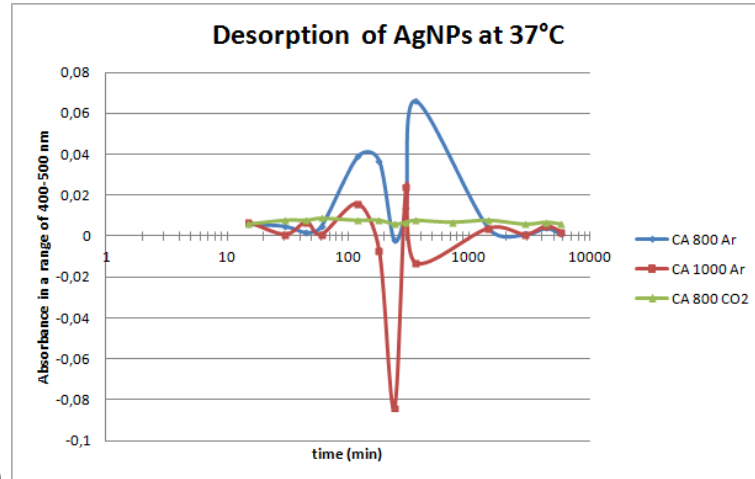
Figure 38: Absorbances as a function of time for the initial solution of 27 ppm of silver nanoparticles containing the different samples of activated carbon.

Observing the different graphs, it can be declared that the adsorption of silver nanoparticles by the samples of activated carbon in function of time is not a linear function. In fact, the absorbances of the solution containing samples of activated carbon carbonized with argon seem to oscillate a lot during the first 24 hours and then they seem to stabilize and start decreasing. For the sample of activated carbon carbonized with CO<sub>2</sub>, during the first three hours, the absorbance was oscillating too but then it started to decrease earlier and faster. This means that as long as the absorbance is oscillating, the samples of activated carbon adsorbed and desorbed silver nanoparticles and then, when the absorbance starts decreasing, the samples were only adsorbing silver nanoparticles. Also, the absorbance measured after 96h of impregnation suggests that the AgNPs adsorption capacity of the samples of activated carbon could be classified that way: AC-800 °C-CO<sub>2</sub> > AC-800 °C-Ar > AC-1000 °C-Ar.

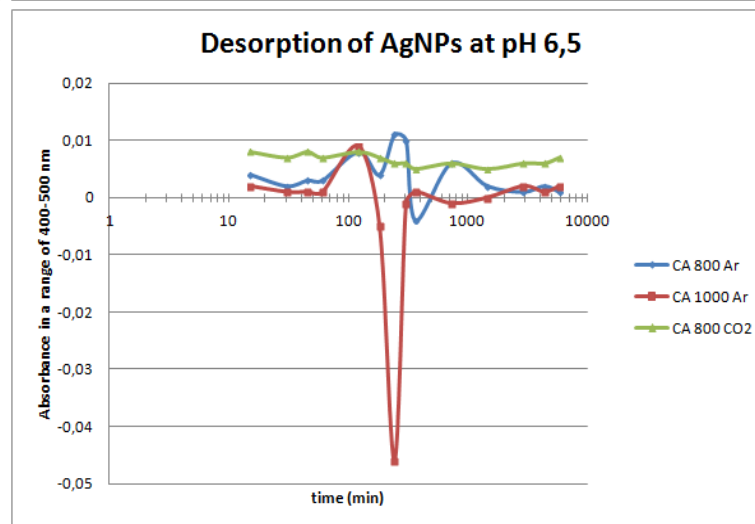
2. Spectrophotometry analysis to see if silver nanoparticles are liberated by activated carbon samples.

Using the same technique, it was also possible to monitor liberation of silver nanoparticles along time in different environmental conditions.

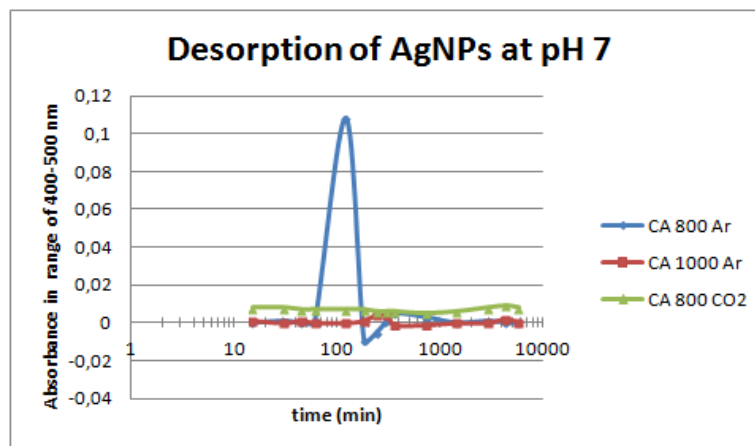




a)



b)



c)



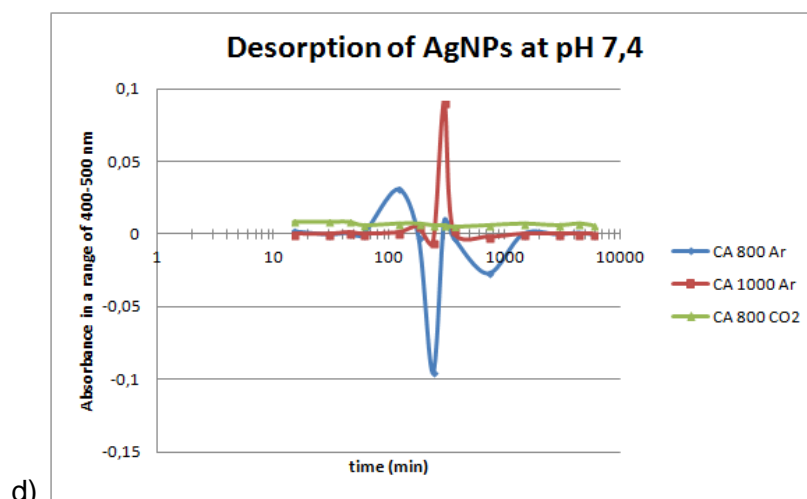


Figure 39: Absorbance as a function of time for physiological solutions containing activated carbon/ AgNPs composite samples at a) 37°C, b) pH 6.5, c) pH 7, d) pH 7.4.

First of all, when the samples were collected, it was visible by eye observation that the solution remains translucent which means that silver nanoparticles weren't liberated in large quantities. With the spectrophotometry results, it can be seen that the maximal absorbance measure was about 0.01 which is really low. For the sample carbonized with CO<sub>2</sub>, no variation is observed in any condition which means that AgNPs weren't liberated at all. For the samples carbonized with argon, in all the different environmental conditions, a small variation of absorbance is observed during the first 24h and after that, the absorbance is constantly null. One possible explanation could be that at some moments during the first 24h (where the absorbance > 0), the samples of activated carbon released a very few silver nanoparticles but once in solution, silver ions complexed with chlorine ions, forming AgCl particles. Then, as the activated carbon shows strong properties of adsorption, the AgCl crystals were adsorb back to the surface of the samples.



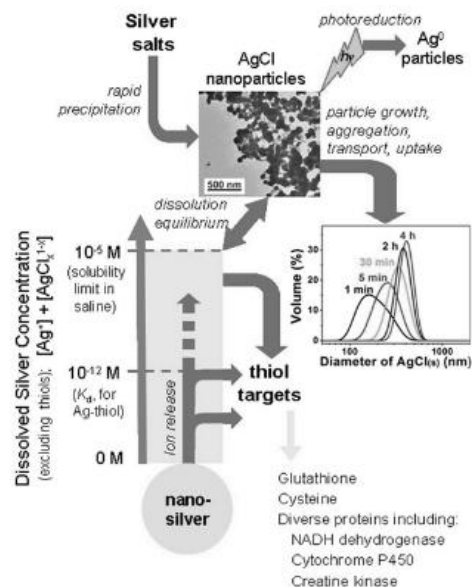


Figure 40: Illustrative scheme explaining the formation of AgCl. Adapted from [48]

Many SEM images with EDX analysis of CA/AgNPs samples showed that silver nanoparticles were interacting with chlorine ions during immersion in physiological solution which reinforce the hypothesis of complexation

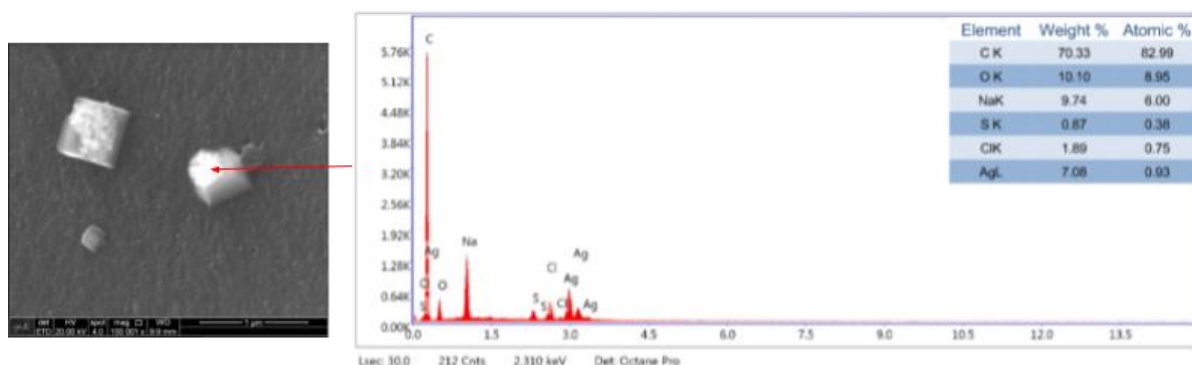


Figure 41: SEM-EDX analysis of CA/AgNPs (81 ppm solution) carbonized at 1000 °C with argon after immersion in physiological solution at 37°C in pH 7.4.

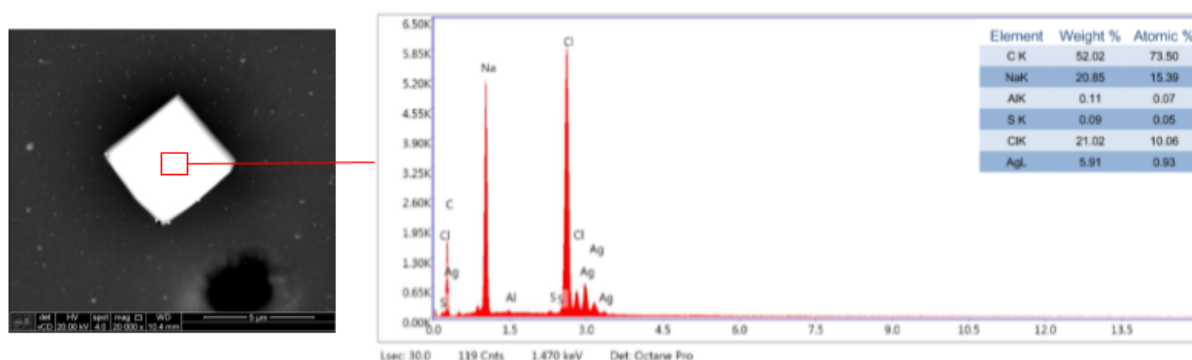


Figure 42: SEM-EDX analysis of CA/AgNPs (54 ppm solution) carbonized at 800 °C with argon after immersion in physiological solution at 37°C in pH 7.4.



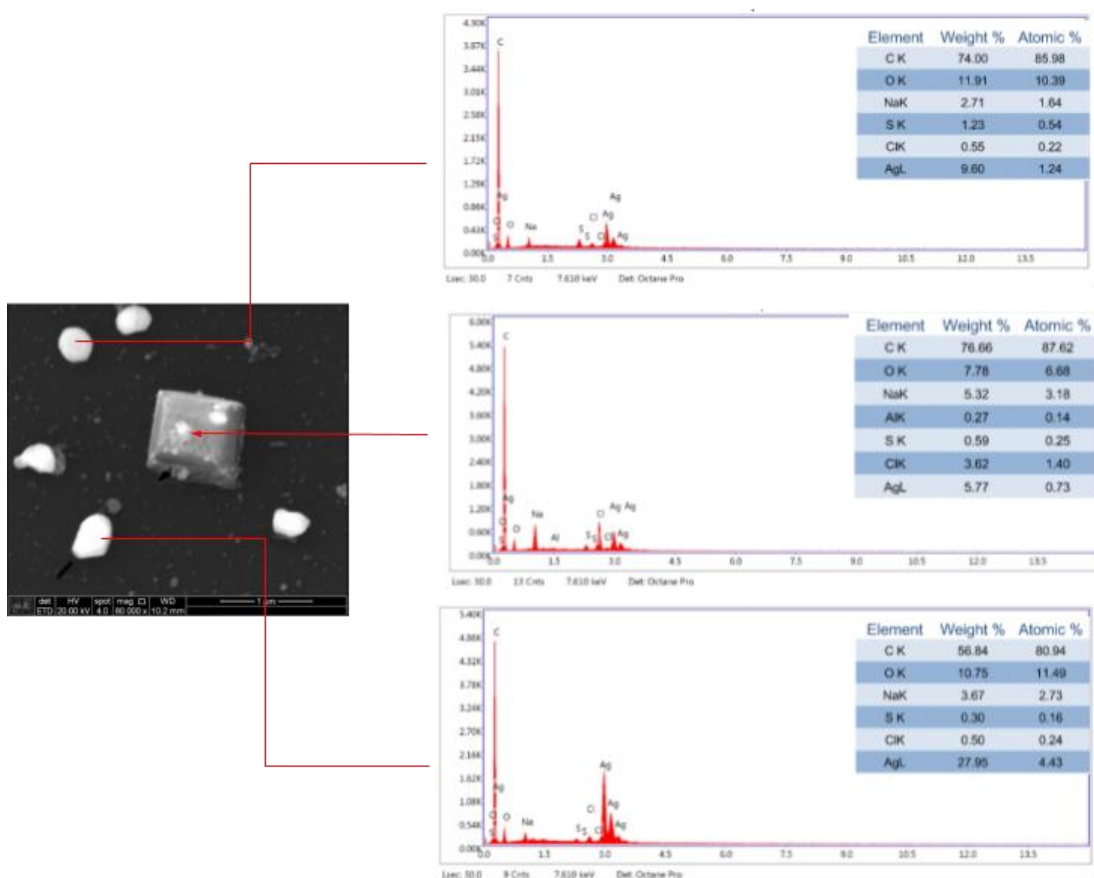


Figure 43: SEM-EDX analysis of CA/AgNPs (81 ppm solution) carbonized at 800 °C with argon after immersion in physiological solution at 37°C in pH 7.4.

As it is shown on the previous figures, it was observed that most of the AgNPs presented sodium and chlorine in their composition and that NaCl crystals present silver in their composition too.

### 3. Analysis of the silver nanoparticles adsorption by activated carbon samples using SEM analysis

Using SEM microscopy and EDX analysis it was possible to optically evaluate the presence of silver nanoparticles on the surface of the activated carbon samples after 5 days of impregnation.



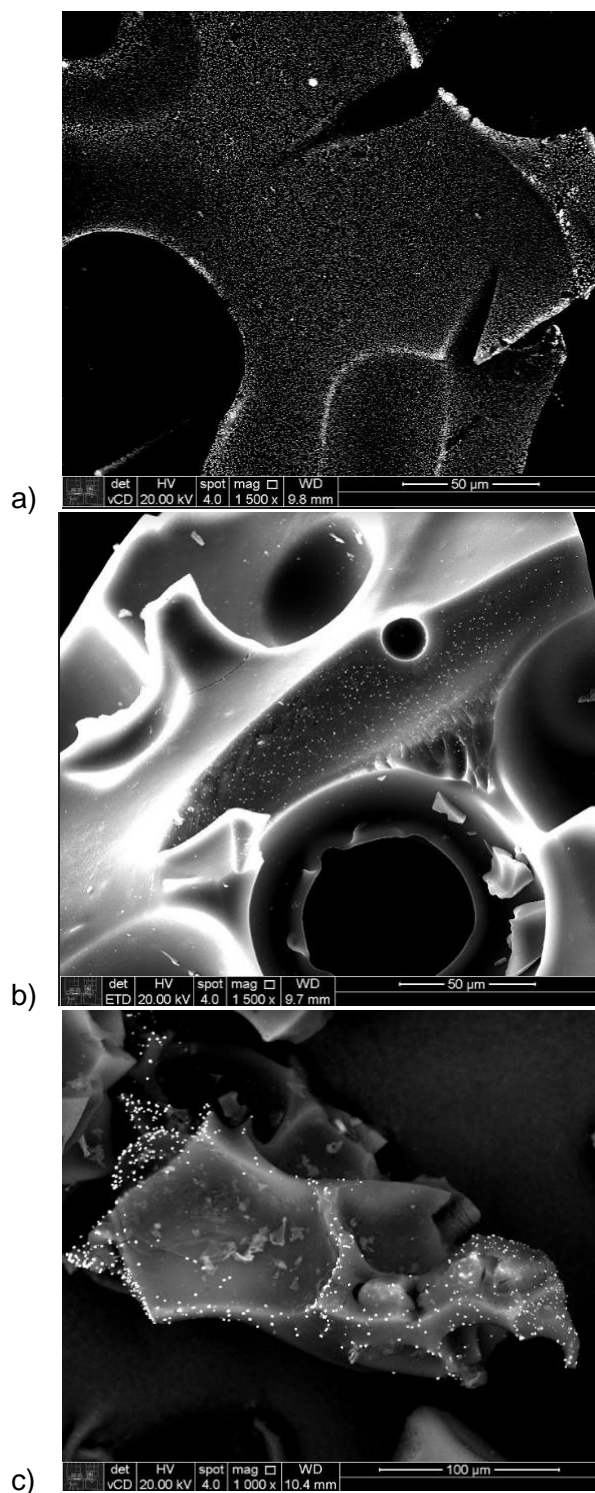


Figure 44: SEM image of activated carbon samples impregnated with 81ppm solution of silver nanoparticles, magnification x 1500, of a) AC-Ar-800 °C ;b) AC-Ar-1000 °C ;c) AC- CO<sub>2</sub>-800 °C.

Thanks to the silver molar mass of 107.87 g/mol , silver nanoparticles are clearly visible using the backscattered electrons detector of the SEM. For these samples, silver nanoparticles solutions of 54ppm and 81ppm were used for the impregnation as the antibacterial efficiency of these solutions have shown better results.



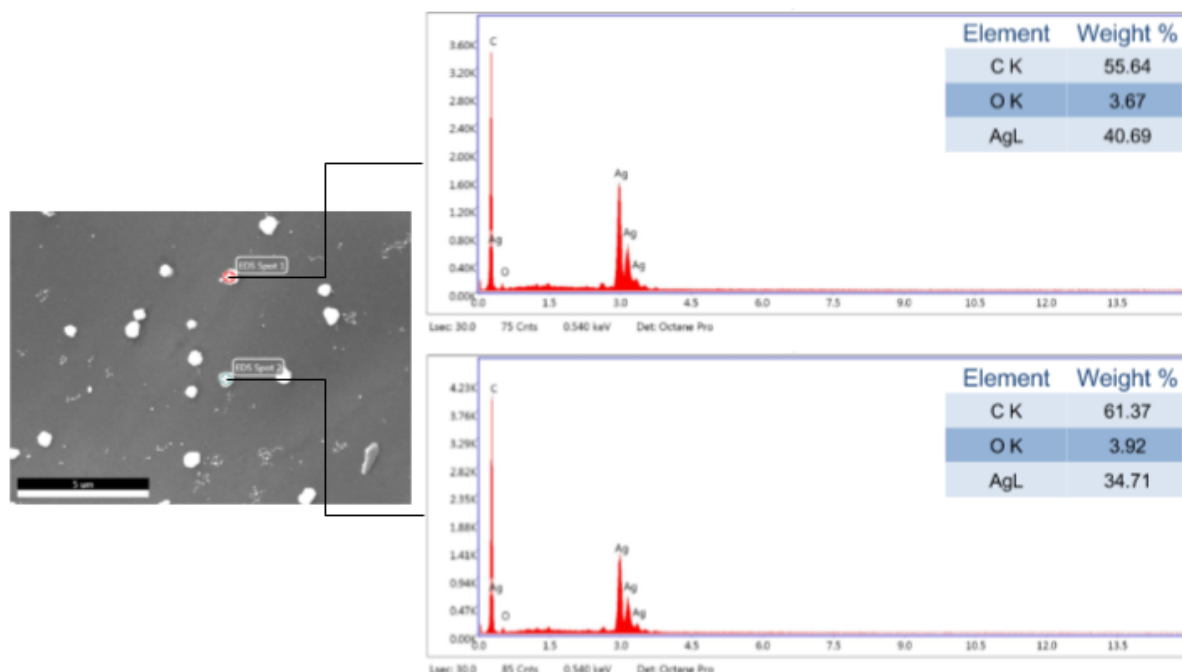


Figure 45: EDX analysis of the AgNPs on the surface of the sample of activated carbon carbonized with argon at 1000 °C impregnated with the 54 ppm solution.

The EDX results for the sample of activated carbon carbonized with argon at 1000°C after impregnation with the 54 ppm solution prove that the white particles are silver nanoparticles. Similar analyses have been realized for all the samples of activated carbon, impregnated with 54 ppm and 81 ppm solutions. In all the samples, the presence of AgNPs has been verified.

In order to evaluate the area occupied by silver nanoparticles and to estimate particle's size, the software Image J has been used. To be able to process the SEM images using the software Image J, the contrast of the SEM images has been increased.



**SEM observations with high contrast after the adsorption of AgNPs by the samples of activated carbon**

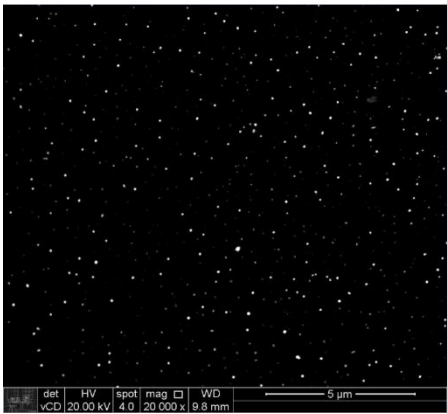
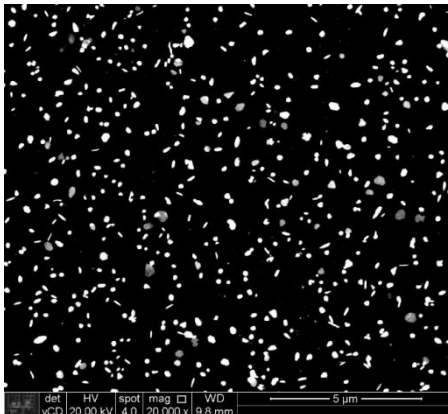
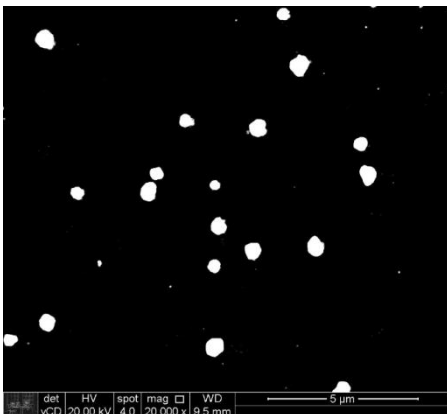
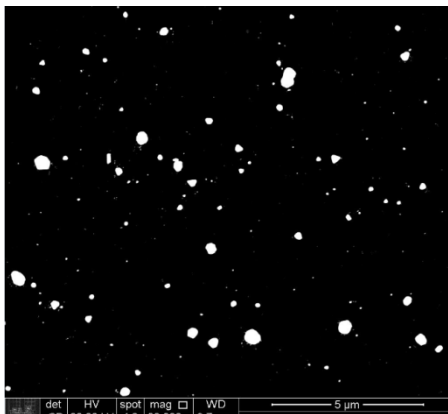
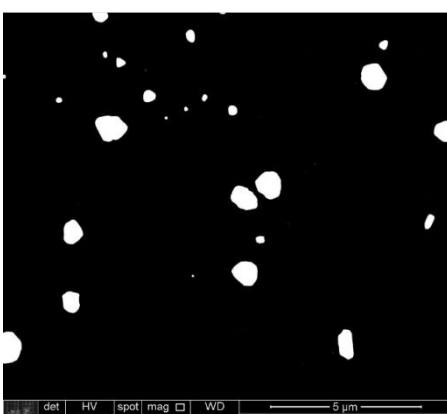
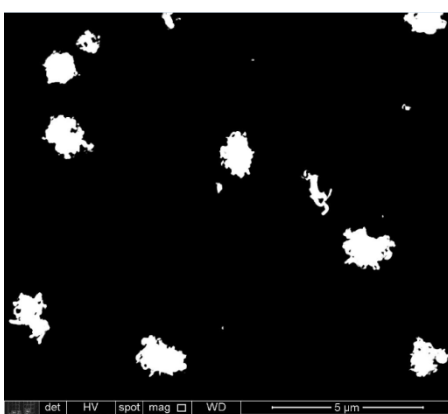
sample (magnitude)	54 ppm solution	81 ppm solution
AC 800 °C/Ar (x 20 000)		
AC 1000 °C/Ar (x 20 000)		
AC 800 °C/CO <sub>2</sub> (x 20 000)		

Table 18: SEM observations with high contrast after the adsorption of AgNPs by the samples of activated carbon.



	54 ppm solution			81 ppm solution		
sample	Area of AgNPs (%)	Average diameter (nm)	Homogeneity of adsorption of AgNPs	Area of AgNPs (%)	Average diameter	Homogeneity of adsorption of AgNPs
AC 800 °C (Ar)	1.59	106.84	yes	9.17	204.35	yes
AC 1000 °C (Ar)	2.52	487.37	no	1.78	178.63	no
AC 800 °C (CO <sub>2</sub> )	2.69	594.31	no	4.14	756.08	no

Table 19: Results of the Image J processing of the SEM images of the activated carbon samples after impregnation with solution of 54 ppm and 81 ppm of silver.

Observing the SEM images, it is clear that both concentration and conditions of carbonization have an impact over adsorption and agglomeration processes of silver nanoparticles.

It was noticed that only the sample carbonized at 800 °C with argon shows a uniform repartition of the silver nanoparticles. The two other samples showed regions with a lot a silver nanoparticles and regions where there were only a few nanoparticles. The results presented in the table above considered places where a lot a nanoparticles were found. So in fact, for the samples impregnated by the 54ppm solution, the sample with the higher percentage of its surface recovered by silver nanoparticles is the sample carbonized with argon at 800 °C and the sample with the lower percentage is the one carbonized with argon at 1000 °C.

When the solution of 81ppm is used for impregnation, the sample of activated carbon carbonized with argon at 800 °C shows way more nanoparticles on its surface and the area occupied by them reaches 9.17%. It can also be observed that some particles are no longer spherical: they form thin crystals of silver. For sample carbonized with CO<sub>2</sub> at 800 °C, in the regions where silver nanoparticles are found, we can see that increasing the concentration of the solution also increase the surface area occupied by silver nanoparticles. For the sample carbonized with argon at 1000 °C, the opposite was observed. The differences observed between the different samples of activated carbon for the same concentration could be explained by a different reactivity and/or different superficial groups between the samples coming from the different conditions of carbonization.



Looking at the average diameter of the silver nanoparticles, huge differences are noticed. When the samples were impregnated with the solution of 54ppm, higher temperature of activation results in larger particles. Also, the use of CO<sub>2</sub> leads to larger particles than with argon. Increasing the concentration of the solution also results in bigger particles except for the sample carbonized with argon at 1000 °C. These observations are linked with the process of agglomeration of silver nanoparticles. To understand better why the particles agglomerate more in some conditions (using CO<sub>2</sub> atmosphere for example) chemical surface analysis of the samples of activated carbon should be done.

#### 4. Antibacterial activity of the activated carbon/ AgNPs composite

##### **Activated carbon impregnated with the solution containing 27ppm of silver nanoparticles**

The antibacterial activity for the different samples of activated carbon impregnated with the AgNPs solution of 27ppm has been studied using tissue culture plate as described before. Following, the tissue culture plate used and its disposition.

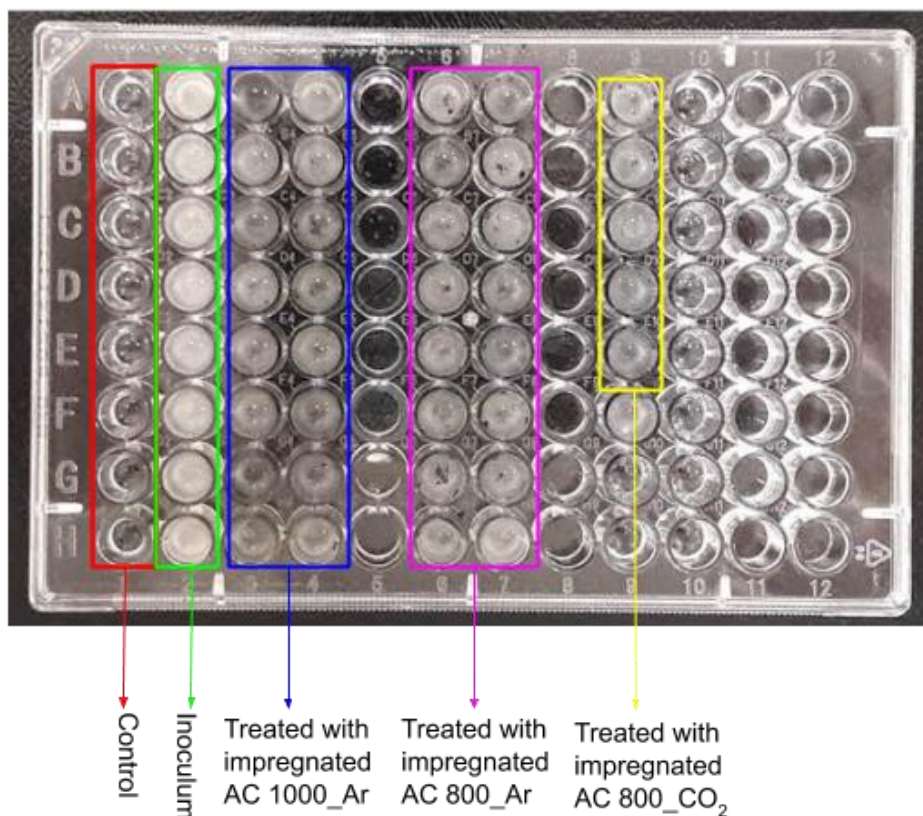


Figure 46: Tissue culture plate used to test activated carbon samples impregnated with the 27 ppm solution.



	1	2	3	4	5	6	7	8	9	10	11	12
A	0,069	0,992	1,627	0,975		1,159	1,673		1,286			
B	0,06	0,948	0,973	1,114		1,319	1,381		1,338			
C	0,055	0,955	1,246	1,468		1,304	1,015		2,16			
D	0,058	0,936	1,008	1,589		1,274	1,295		1,684			
E	0,055	0,926	1,298	1,209		1,29	1,293		1,331			
F	0,056	0,927	1,12	1,603		1,443	1,216		1,172			
G	0,053	0,905	1,897	1,185		1,088	1,154					
H	0,052	0,983	1,125	0,883		1,098	0,997					

Figure 47: Spectrophotometry results of the tissue culture plate used to test activated carbon samples impregnated with the 27 ppm solution.

For the analysis of the bactericidal efficiency of the samples of activated carbon impregnated with AgNPs, the analysis by spectrophotometry was inappropriate. Indeed, the samples of activated carbon absorb a lot and calculi of reduction of bacterial growth using the absorbance results are not possible. Nevertheless, it can be observed that the cavities are less turbid which mean that there is a real reduction of bacterial growth. To be able to estimate this reduction in numbers, some methods that count the number of colonies forming unit (CFU) of bacteria are possible to apply.

### **Activated carbon impregnated with the solution containing 54 ppm and 81 ppm of silver nanoparticles**

As the antibacterial tests showed better results for the solutions of 54 ppm and 81ppm, it was decided to use these concentrations for impregnation to then verify the antibacterial activity using tissue culture plate.



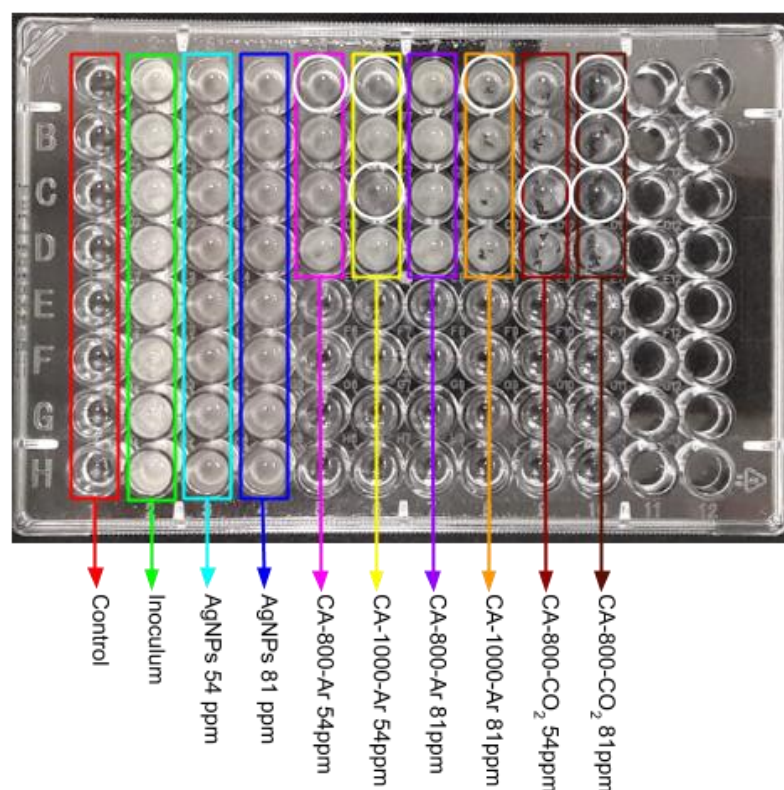


Figure 48: Tissue culture plate used to test activated carbon samples impregnated with the 54 ppm and 81ppm solution.

	1	2	3	4	5	6	7	8	9	10	11	12
A	0,077	1,037	0,97	0,882	0,693	0,463	1 068	1,231	1,235	1,241		
B	0,069	0,983	0,773	0,77	0,89	0,825	1,049	1,077	0,918	1,122		
C	0,062	1,081	0,731	0,662	0,812	0,325	0,869	0,924	0,931	1,7		
D	0,064	0,952	0,646	0,649	0,758	0,757	0,887	0,925	0,792	1,406		
E	0,063	0,919	0,665	0,675								
F	0,066	0,893	0,592	0,589								
G	0,066	0,873	0,682	0,684								
H	0,1	0,911	0,664	0,63								

Figure 49: Spectrophotometry results of the tissue culture plate used to test activated carbon samples impregnated with the 54 ppm and 81 ppm solution.

This time, the bacterial growth was reduced by 25.15% with the 54ppm concentrated solution and by 27.56 wt.% with the 81ppm concentrated solution. These results show lower efficiency than the previous tests even if the solutions were the same.

For the cavities with activated carbon, the results of spectrophotometry are still not exploitable but it is clear that there is a bacterial growth reduction as the cavities



are less turbid than the inoculum. The cavities circled in white seem to have the best results. Between all these cavities, the ones with activated carbon sample carbonized at 800 °C with CO<sub>2</sub> and impregnated by the 81 ppm solution are the more translucent which mean that they have the best efficiency against bacterial growth. At the contrary, the cavities with activated carbon carbonized at 800 °C with argon and impregnated by the 81ppm solution are as turbid as the inoculum which means that this sample is not efficient against bacterial growth. This last result can be related to the form of the particles formed in these conditions of carbonization and impregnation. As it was already described before, thin crystals of silver were formed.

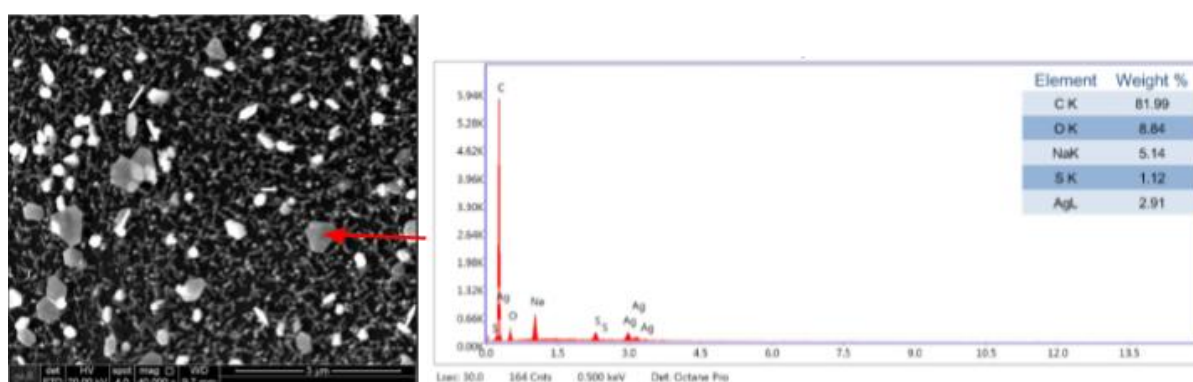


Figure 50: SEM image of activated carbon carbonized at 800 °C with argon and impregnated by the 81 ppm solution. Magnification x 40 000.

Along time, it is probable that the nanoparticles agglomerate to form these silver crystals and then these crystals join themselves to form a film. As crystals possess stronger bounds, it is possible that the liberation of silver ions doesn't occur, and the composite is not effective against bacterial growth.



## IV. Discussion of the results

The different carbonizations in different conditions of temperature and atmosphere, suggested that pore size increases with temperature of activation which is also verified in many articles [49-51]. It is also referred in many articles that the  $\text{CO}_2$  reacts with the carbon during the activation process and consequently, an enlargement of the pores is observed [50-52] which confirm the observations. Some studies [53] comment that oxygen surface groups on carbon decompose at different temperatures which could explain the results of the experiment which suggest that higher temperature leads to lower quantity of oxygen.

The resultant macroporous structures obtained with different conditions of carbonization correspond to the expectations: indeed, macroporous structure is required for cell ingrowths. In the literature, it is said that diameter range of 12-50  $\mu\text{m}$  is adapted for fibrovascular growth, of 50-150  $\mu\text{m}$  is adapted for osteoid formation and that over 150  $\mu\text{m}$  is adapted for the ingrowth of mineral bone [38].

The synthesized nanoparticles have different size diameters: on the distribution, the more intense peak were around 33 nm and the other particles showed diameter between 1nm and 10 nm. In the reference paper used for the synthesis [46], the silver nanoparticles solution is also yellow but has nanoparticles with a diameter about 20 nm with is smaller than the results obtained. This could be explained by the fact that silver nitrate were substituted by silver acetate. Many articles proved that the precursor used for the synthesis has an influence over particle size [54-55].

During the monitoring of adsorption of AgNPs, it was found that the adsorption starts to be effective after 24 hours for the samples carbonized with argon and after 3 hours for the sample carbonized with  $\text{CO}_2$ . In the literature [56], a similar experiment have been realized in order to monitor Ag(I) removal using different carbonaceous materials, and it was found that most of the adsorption was occurring during the five first hours. Of course, the conditions of the experiment (the media of adsorption for example) are not the same so it is not impossible to compare the results, but it can be said that adsorption of Ag(I) and adsorption of AgNPs have different kinetics. It is also important to remember that AgNPs are coated with PVA which probably interferes during the adsorption process.



It was also observed that after impregnation in AgNPs solutions, depending of the activated carbon sample and of the concentration of AgNPs in solution, the particles have a larger diameter which is characteristic of agglomeration process. This observation is not clearly understood but some researchers noticed that in carbon matrix, silver nanoparticles tend to be agglomerated [57] which confirms that the activated carbon sample plays a role in agglomeration process. Also, the role of the capping agent in agglomeration process is already set as the polymer coating might become unstable and dissolve [58] so as the solution gets older, agglomeration can be observed. And finally, some articles affirm [58] that the aggregation and sedimentation of nanoparticles depend of the type and number of ions present in the solution which could help to explain the differences observed when using different concentrations of AgNPs during the impregnation step.

When the impregnated samples were put in physiological media in different conditions of temperature and pH, during the first 24 hours, in some samples, a very small oscillation of absorbance, characteristic of an oscillation between liberation and adsorption processes, was observed. In the literature [48], it is said that O- and N-containing polymers coating can delay and extend ion release by accumulating and release inventories of bound  $\text{Ag}^+$ . As the formula of PVA contain oxygen  $((\text{CH}_2\text{CHOH})_n)$ , it could explain this oscillation. After 96 hours, it was observed that there was no silver in the solution. In the literature [48,59-60], we can found that silver ion release decrease with the  $\text{Cl}^-$  concentration in the solution and that  $\text{Cl}^-$  can co-precipitate  $\text{Ag}^+$  forming  $\text{AgCl}$ . These affirmations confirm that AgNPs interact with the chlorine ions of the physiological solution and also could explain why silver ions release is low and even null after 96 hours.

The antibacterial results obtained with different solutions of AgNPs differ depending on the experiment. Consequently, it is difficult to draw a precise conclusion. However, it is clear that all the silver nanoparticles solutions are efficient against bacterial growth and it seems that higher concentration leads to higher inhibition. In the literature, it can be found that AgNPs are toxic for eukaryotic organism at the concentrations higher than 30ppm [61]. Another article showed that concentration of 10 ppm show efficient antibacterial activity against *E.Coli* [62]. These data justify that during the experiment, concentrations of 27ppm, 54ppm and 81ppm partially inhibited bacterial growth. However, the experiment didn't reach 100% of



inhibition as it can be observed in the literature. To understand better the antibacterial efficiency of the AgNPs synthesized, a better characterization is required. It has already been proved that size, shape and distribution of AgNPs have a real influence on the antibacterial properties [63-65]. The truncated triangular silver nanocrystals observed after impregnation with 81ppm solution of the activated carbon carbonized at 800 °C with argon, are proved to be metallic silver particles crystallized in the face-centered cubic (fcc) structure with basal {111} lattice planes [64,66-67]. In regard to the bacterial efficiency of the different composite of CA/AgNPs, it is clear that they have a positive impact on bacterial growth inhibition, but it was difficult to characterize this reduction. To characterize this reduction, it will be necessary to count the colony forming units of bacteria. However, we can suppose that the silver nanoparticles on the surfaces of activated carbon samples are liberating silver ions which have a bactericidal effect [68].



## V. Conclusion

First of all, activated carbon was successfully synthesized using pure black liquor as a precursor. Also, the addition of PMMA permitted to obtain appropriate macroporous structures for cell growth and vascularization after carbonization. It has been seen that both temperature and atmosphere used during carbonization have an influence over the structure and the composition of the material. Higher temperature leads to larger pores and higher purity as some components of black liquor only volatilize if the carbonization is realized at 1000 °C. Using CO<sub>2</sub>, a strong interaction between the gas and the carbon of the sample was observed. Indeed, the CO<sub>2</sub> reacts with C forming CO(g) and this reaction leads to bigger pores and possibly to the creation of nanoporous.

Then, the synthesis of silver nanoparticles was successfully realized with a chemical reduction using silver acetate as a precursor, borohydride as a reductor agent and PVA as a stabilizer. For the implementation of silver nanoparticles on the surface of activated carbon, the samples were immersed in silver nanoparticles solutions and adsorption processes were sufficient to bind the silver nanoparticles on the surface. After microscope observation, it was proved that all the samples had silver nanoparticles on their surfaces. However, it was observed that the conditions of carbonization have an important influence over the absorption process of silver nanoparticles. Moreover, it was clear that the concentration of the silver nanoparticles solution also influences the processes of adsorption and aggregation of silver nanoparticles. To be able to understand these differences, a better characterization of the surface chemistry of the samples of activated carbon is required.

Finally, during the antibacterial tests against *E.Coli*, the solutions of silver nanoparticles and the composites of CA/AgNPs have shown to be efficient against the bacteria growth. To characterize this reduction, it will be necessary to count the colony forming units.

To conclude, all these results are encouraging to continue the investigation over composites of activated carbon with silver nanoparticles for future uses in bone regeneration applications.



## Bibliography

- [1]. AMARAL-LABAT, Gisele.. Educational material talking about activated carbon as a part of a course about technology of composites.
- [2]. MOSELEY, Patrick T., RAND, David A.J., DAVIDSON, Alistair., *et al.* Understanding the functions of carbon in the negative active-mass of the lead–acid battery: A review of progress. *Journal of energy storage*, 2018, vol.19, p.272-290.
- [3]. SUHAS, CARROTT, P.J.M., RIBEIRO CARROTT, M.M.L.. Lignin – from natural adsorbent to activated carbon: A review. *Bioresource Technology*, 2007, vol. 98, n°12, p.2301-2312.
- [4]. KANIA, Nicolas., *Utilisations de charbons actifs dans des procédés d'adsorption de composés organiques volatils et des procédés de catalyse dans l'eau*. Doctoral thesis in organic and macromolecular chemistry, with Eric Monflier and Anne Ponchel as supervisors, 2010.
- [5]. ZHAO, Ying., Wang, Zi-Qiang., ZHAO, Xin., *et al.* Antibacterial action of silver-doped activated carbon prepared by vacuum impregnation. *Applied surface science*, 2013, vol. 266, p.67-72.
- [6]. RAGAN, Steve., MEGONNELL, Neal. Activated carbon from renewable resources - Lignin. *Cellulose chemistry and technology*, 2011, vol.45, n°7-8, p.527-531.
- [7]. AMARAL-LABAT, Gisele., BRAGHIROLI, Flavia Lega., BOSS, Alan F.N., *et al.* *Converting Cellulose's Raw Black Liquor into Activated Porous Carbon: A Synthesis Routine to Control Final Product Properties*.
- [8]. XIA, Changlei., SHI, Sheldon Q.. Self activation for activated carbon from biomass: theory and parameters. *Green Chemistry*, 2015, vol.18, n°7.
- [9].CHEMVIRON, company website.  
Available on: <<https://www.chemviron.eu/products/activated-carbon/>>.
- [10]. MARKETSANDMARKETS, Activated carbon market, 2017, page report 181.  
Available on: <<https://www.marketsandmarkets.com/Market-Reports/activated-carbon-362.html>>.
- [11]. LI, Wen-Ru., XIE, Xiao-Bao., SHI, Qing-Shan., *et al.* Antibacterial activity and mechanism of silver nanoparticles on *Escherichia coli*, *Applied microbial and cell physiology*, 2010, n°85, p.1115-1122.



- [12]. AMARAL-LABAT, Gisele. Electronic publication [composition of black liquor]. E-mail received from <gisele.amaral@usp.br> on the 01/04/2019.
- [13]. WITZLER, Markus., ALZAGAMEEM, Aba., BERGS, Michel., *et al.* Lignin-derived biomaterials for drug release and tissue engineering. *Molecules*, 2018, vol.23, n°1885.
- [14]. FERNANDES, Emanuel. M., PIRES, Ricardo. A., MANO, Juan. F., *et al.* Bionanocomposites from lignocellulosic resources: Properties, applications and future trends for their use in the biomedical field. *Progress in polymer science*, 2013, vol. 38, n°10-11, p.1415-1441.
- [15]. EL-NOUR, Kholoud M.M.A., EFTAIHA, Ala'a., AL-WARTHAN, Abdulrhman.,*et al.* Synthesis and application of silver nanoparticles. *Arabian journal of chemistry*, 2010, vol.3, p.135-140.
- [16]. CHEN,X., SCHLUESENER, H.J. Nanosilver: A nanoprodut in medical application. *Toxicology letters*, 2008, vol.176, p.1-12.
- [17]. XU, Hengyi., QU, Feng., XU, Hong., *et al.* Role of reactive oxygen species in the antibacterial mechanism of silver nanoparticles on *Escherichia coli* O157:H7, *Biomaterials*, 2006, vol.19, n°2.
- [18]. Feng, Q.L., Wu, J., CHEN, G.Q., *et al.* A mechanistic study of the antibacterial effect of silver ions on *Escherichia coli* and *Staphylococcus aureus*, *Journal of biomedical materials research*, 2000, vol. 52, n°4, p.662-668.
- [19]. AKTER, Mahmuda., SIKDER, Md. Tajuddin., RAHMAN, Md. Mostafizur.,*et al.* A systematic review on silver nanoparticles-induced cytotoxicity: Physicochemical properties and perspectives. *Journal of advanced research*, 2018, vol.9, p.1-16.
- [20]. RODRIGUEZ-SANCHEZ, L., BLANCO, M. C., LOPEZ-QUINTELA, M. A.. Electrochemical synthesis of silver nanoparticles, *Journal of Physical Chemistry B*, 2000, n°104, p.9683-9688.
- [21]. YIN, Bingsheng., MA, Houyi., WANG, Shuyun., *et al.* Electrochemical Synthesis of Silver Nanoparticles under Protection of Poly (N- vinylpyrrolidone), *Journal of Physical Chemistry B*, 2003, n°107, p.8898-8904.
- [22]. STAROWICZ, Maria., STYPULA, Barbara., BANAS, Jacek.. Electrochemical synthesis of silver nanoparticles, *Electrochemistry Communications* 8, 2006, p.227-230.



- [23]. DURAN, Nelson., DURAN, Marcela., BISPO DE JESUS, Marcelo., *et al.* Silver nanoparticles: A new view on mechanistic aspects on antimicrobial activity. *Nanomedicine: Nanotechnology, Biology, and Medicine*, 2016, vol.12, p.789-799.
- [24]. ZHANG, Xi-Feng., LIU, Zhi-Guo., SHEN, Wei., *et al.* Silver nanoparticles: Synthesis, Characterization, Properties, Applications, and Therapeutic Approaches. *International journal of molecular sciences*, 2016, review.
- [25]. CHEN,X., SCHLUESENER, H.J. Nanosilver: A nanoproduct in medical application. *Toxicology letters*, 2008, vol.176, p.1-12.
- [26]. DE JONG, Wim. H., BORM, Paul. JA.. Drug delivery and nanoparticles: Applications and hazards, *International Journal of Nanomedicine*, 2008, vol.3, n°2, p.133-149.
- [27]. LIU, Jingyu, SONSHINE, David. A., SHERVANI, Saira., *et al.* Controlled release of biologically active silver from nanosilver surfaces, *ACS Nano*, 2010, vol. 4, n°11, p.6903-6910.
- [28]. LIU, Jingyu., HURT, Robert. H.. Ion release and particle persistence in aqueous nano-silver colloids, *Environmental Science & Technology*, 2010, n°44, p.2169-2175.
- [29]. DAMM, C., MÜNESTEDT, H.. Kinetic aspects of the silver ion release from antimicrobial polyamide/ silver nanocomposites, *Applied Physics A*, n°91, p.479-486.
- [30]. AUFFAN, Mélanie., ROSE, Jérôme., BOTTERO, Jean-Yves., *et al.* Towards a definition of inorganic nanoparticles from an environmental, health and safety perspective, *Nature nanotechnology*, 2009, n°4, p.634-641.
- [31]. MAQUSOOD, Ahamed., ALSALHI, Mohamad. S., SIDDIQUI, M.K.J.. Silver nanoparticle applications and human health, *Clinica Chimica Acta*, 2010, n°411, p.1841-1848.
- [32]. Hollister, S.J.: Porous scaffold design for tissue engineering. *Nature Materials*, n°4, p.518-524.
- [33]. FURTH, Mark. E., ATALA, Anthony., VAN DYKE, Mark. E.. Smart biomaterials design for tissue engineering and regenerative medicine. *Biomaterials*, 2007, n°28, p. 5068-5073.
- [34].ZHANG, R., MA, PX.. Poly(alpha-hydroxy acids)/hydroxyapatite porous composites for bone-tissue engineering. I.Preparation and morphology. *Journal of Biomedical Materials Research*, 1999, n°44, p.446-455.



- [35]. RAMIER, Julien.. Structures poreuses tridimensionnelles de biopolymères pour l'ingénierie tissulaire. Autre. Université Paris-Est, 2012. French.
- [36]. SHI, Yanni., HAN, Hoa., QUAN, Haïyu., *et al.* Activated carbon fibers/poly(lactic-co-glycolic) acid composite scaffolds: Preparation and characterizations. *Materials Science and Engineering C* , 2014, n°43, p. 102-108.
- [37]. MENAA, Farid., ABDELGHANI, Adnane., MENAA, Bouzid.. Graphene nanomaterials as biocompatible and conductive scaffolds for stem cells: impact for tissue engineering and regenerative medicine. *Journal of tissue engineering and regenerative medicine*, 2015, n°9, p.1321-1338.
- [38]. PETITE, Herve., VIATEAU, Véronique., BENSAID, Wassila., *et al.* Tissue-engineered bone regeneration. *Nature Biotechnology*, 2000, vol.18, n°9, p.959-963.
- [39]. LISOWSKA, B., KOSSON, D., DOMARACKA, K.. Lights and shadows of NSAIDS in bone healing; the role of prostaglandins in bone metabolism, *Drug design, development and therapy*, 2018, n°12, p.1753-1758.
- [40]. MOHAMMED, Azad., ABDULLAH, Avin.. Scanning Electron Microscopy (SEM) : A REVIEW. In: PROCEEDINGS OF 2008 INTERNATIONAL CONFERENCE ON HYDRAULICS AND PNEUMATICS- HERVEX, 24., 2018, Baile Govora. Available on: <<http://www.fluidas.ro/hervex/proceedings/proceedings2018.pdf>>.
- [41]. INKSON, B. J.. Scanning electron microscopy (SEM) and transmission electron microscopy (TEM) for materials characterization. *Materials characterization using nondestructive evaluation (NDE) methods*, 2016, p.17-43.
- [42]. CHEMISTRY LIBRETEXT, VO, Kevin., *Spectrophotometry in Physical and theoretical chemistry*, California, 2019. Available on: [https://chem.libretexts.org/Bookshelves/Physical\\_and\\_Theoretical\\_Chemistry\\_Textbook\\_Maps/Supplemental\\_Modules\\_\(Physical\\_and\\_Theoretical\\_Chemistry\)/Kinetics/Reaction\\_Rates/Experimental\\_Determination\\_of\\_Kinetics/Spectrophotometry](https://chem.libretexts.org/Bookshelves/Physical_and_Theoretical_Chemistry_Textbook_Maps/Supplemental_Modules_(Physical_and_Theoretical_Chemistry)/Kinetics/Reaction_Rates/Experimental_Determination_of_Kinetics/Spectrophotometry)
- [43]. RETSCH TECHNOLOGY, *Dynamic light scattering for particle size measurement on the nanometer scale*, Germany, 2019. Available on: <https://www.retsch-technology.com/applications/technical-basics/dynamic-laser-light-scattering/>
- [44]. STETEFELD, Jorg., McKENNA, Sean., PATEL, Trushar R.. Dynamic light scattering: a practical guide and applications in biomedical sciences. *Biophysical Reviews*, 2016, p.409-427.



- [45]. MALVERN, Dr. Ryan Shaw, Dynamic Light Scattering Training Achieving reliable nano particle sizing, Australia, 2019. Available on: <http://149.171.168.221/partcat/wp-content/uploads/Malvern-Zetasizer-LS.pdf>
- [46]. ALVES MELO Jr., M., SOARES SANTOS, L.S. *et al.* Preparação de nanopartículas de prata e ouro: um método simples para a introdução de nanociência em laboratório de ensino. *Química Nova*, 2012, vol.35, nº9.
- [47]. ZHOU, Kui., DONG, Chunfa., ZHANG, Xianglin., *et al.* Preparation and characterization of nanosilver-doped porous hydroxyapatite scaffolds. *Ceramics international*, 2015, vol.41, nº1, p.1671-1676.
- [48]. LIU, Jingyu., SONSHINE, David. A., SHERVANI, Saira., *et al.* Controlled release of biologically active silver from nanosilver surfaces. *ACS Nano*, 2010, vol. 4, nº 11, p. 6903-6913.
- [49]. SUN, Y., ZHANG, J-P., YANG, G., *et al.* Preparation of activated carbon with large specific surface area from reed black liquor. *Environmental Technology*, 2007, vol. 28, p.491-497.
- [50]. ZHANG, Tengyan., WALAWENDER, Walter. P., FAN, L.T. *et al.* Preparation of activated carbon from forest and agricultural residues through CO<sub>2</sub> activation, *Chemical Engineering Journal*, 2004, nº105, p.53-59.
- [51]. BERGNA, D., HU, T., PROKKOLA, H., *et al.* Effect of some process parameters on the main properties of activated carbon produced from peat in a lab-scale process, *Waste and Biomass Valorization*, 2019. Available on: <https://link.springer.com/article/10.1007/s12649-019-00584-2>
- [52]. MOLINA-SABIO, M., GONZALES, M. T., RODRIGUEZ-REINOSO, F., *et al.* Effect of steam and carbon dioxide activation in the macropore size distribution of activated carbon, *Carbon*, 1995, vol. 34, nº4, p. 505-509.
- [53]. BARTON, S. S., GILLESPIE, D., HARRISON, B. H.. Surface Studies of carbon: acidic oxides on spheron 6, *Carbon*, 1973, vol. 11, p. 649-654.
- [54]. HIRAMATSU, Hiroki., OSTERLOH, Frank. E.. A simple large-scale synthesis of nearly monodispersed gold and silver nanoparticles with adjustable sizes and with exchangeable surfactants. *Chemistry of Materials*, 2004, vol. 16, nº 13.



- [55]. ZIELINSKA, Anna., SKWAREK, Ewa., ZALESKA, Adriana., *et al.* Preparation of silver nanoparticles with controlled particle size. *Procedia Chemistry*, 2009, n°1, p. 1560-1566.
- [56]. HANZLIK, J., JEHLICKA, Jan., SEBEK, Ondrej., *et al.* Multi-component adsorption of Ag(I), Cd(II) and Cu(II) by natural carbonaceous materials. *Water Research*, 2004, vol. 38, n°8, p. 2178-2184.
- [57]. MORONES, Jose. Ruben., ELECHIGUERRA, Jose. Luis., CAMACHO, Alejandro., *et al.* The bacterial effect of silver nanoparticles. *Nanotechnology*, 2005, n°16, p. 2346- 2353.
- [58]. STEBOUNOVA, Larissa. V., GUIO, Ethan., GRASSIAN, Vicki. H.. Silver nanoparticles in simulated biological media: a study of aggregation, sedimentation, and dissolution. *Journal of Nanoparticles Research*, 2011, n°13, p. 233-244.
- [59]. ZHANG, Hongyin., SMITH, James. A., OYANADEL-CRAVER, Vinka.. The effect of natural water conditions on the anti-bacterial performance and stability of silver nanoparticles capped with different polymers. *Water research*, 2012, n°46, p. 691-699.
- [60]. REIDEY, Bogumila., HAASE, Andrea., LUCH, Andreas., *et al.* Mechanisms of silver nanoparticle release, transformation and toxicity: A critical review of current knowledge and recommendations for future studies and applications. *Materials*, 2013, n°6, p.2295-2350.
- [61]. KVITEK, L., PANACEK, A., PRUCEK, R., *et al.* Antibacterial activity and toxicity of silver - nanosilver versus ionic silver. *Journal of Physics: Conference Series*.
- [62]. LI, Wen-Ru., XIE, Xiao-Bao., SHI, Qing-Shan., *et al.* Antibacterial activity and mechanism of silver nanoparticles on *Escherichia coli*, *Applied microbiology and biotechnology*, 2010, vol. 85, n° 4, p. 1115-1122.
- [63]. PAL, Sukdeb., TAK, Yu Kyung., SONG, Joon Myong.. Does the antibacterial activity of silver nanoparticles depend on the shape of the nanoparticles? A study of the Gram-Negative Bacterium *Escherichia coli*. *Applied and environmental microbiology*, 2007, vol. 73, n° 6, p. 1712-1720.



[64]. DONG, Pham Van., HA, Chu Hoang., BINH, Le Tran., *et al.* Chemical synthesis and antibacterial activity of novel-shaped silver nanoparticles. *International Nano Letters*, 2012, vol. 2, n° 9.

[65]. GAO, HONGFANG, HUI, *et al.* Controllable preparation and mechanism of nano-silver mediated by the microemulsion system of the clove oil. *Results in Physics*, 2017, vol. 17, p. 3130-3136.

[66]. DJAFARI, Jamila., FERNANDEZ-LODEIRO, Carlos., FERNANDEZ-LODEIRO, Adrian., *et al.* Exploring the control in antibacterial activity of silver triangular nanoplates by surface coating modulation. *Frontiers in Chemistry*, 2019.

[67]. KLAUS, Tanja., JOERGER, Ralph., OLSSON, Eva., *et al.* Silver-based crystalline nanoparticles, microbially fabricated. *Proceedings of the national academy of sciences of the United State of America*, 1999, vol. 96, n° 24, p. 13611-13614.

[68]. ZHANG, Tianlu., WANG, Liming., CHEN, Qiang., *et al.* Cytotoxic Potential of Silver Nanoparticles. *Yonsei Medical Journal*, 2014, n°55, p.283-291.